Anisotropic fast-marching on cartesian grids using Voronoi's first reduction of quadratic forms

Jean-Marie Mirebeau

Anisotropic fast-marching on cartesian grids using Voronoi's first reduction of quadratic forms

Jean-Marie Mirebeau*

April 12, 2017

Abstract

We address the numerical computation of distance maps with respect to Riemannian metrics of strong anisotropy. For that purpose we solve generalized eikonal equations, discretized using adaptive upwind finite differences on the cartesian grid, via a variant of the fast marching algorithm. The key ingredient of our PDE numerical scheme is Voronoi's first reduction, a tool from discrete geometry which characterizes the interaction of a quadratic form with an additive lattice.

Two variants of the introduced scheme are also presented, adapted to sub-Riemannian and to Rander metrics respectively, which can be regarded as degenerate Riemannian metrics and as Riemannian metrics perturbed with a drift term respectively. We establish the convergence of the proposed scheme and of its variants, with convergence rates. Numerical experiments illustrate the effectiveness of our approach in various contexts, in dimension up to five, including an original sub-Riemannian model related to the penalization of path torsion. The proposed numerical scheme shows good behavior with Riemannian metrics of condition numbers of 10 and more, can be enhanced by the use of second order finite differences, and is easier to implement, generalize, and up to 5 times faster than previous semi-Lagrangian discretization [18].

Keywords: Riemannian metric, Sub-Riemannian metric, Rander metric, Eikonal equation, Viscosity solution, Fast Marching Method, Voronoi Reduction.

1 Introduction

In this paper, we develop a new and efficient numerical method for the computation of distance maps with respect to anisotropic Riemannian metrics, sub-Riemannian metrics and Rander metrics. For that purpose we discretize generalized eikonal equations, also called static first order Hamilton Jacobi Bellman (HJB) Partial Differential Equations (PDEs), on a cartesian grid. Our approach relies on a special representation of the Hamiltonian, via upwind finite finite differences on an adaptive stencil, which is designed using Voronoi's first reduction of quadratic forms [26] - a tool from discrete geometry mostly known for its application in the study sphere packings and in number theory. For this reason, the method is referred to as Fast-Marching using Voronoi's First Reduction (FM-VR1).

Before entering the details of the addressed PDEs and of their discretisations, let us mention some of the potential applications. The standard eikonal equation is $\|\mathrm{d}u\| = f$, where $\mathrm{d}u$

*University Paris-Sud, CNRS, University Paris-Saclay, 91405, Orsay, France
This work was partly supported by ANR young researcher grant NS-LBR ANR-13-JS01-0003-01

denotes the differential of u, on a domain of $\mathbb{R}^d$ and with suitable boundary conditions. This PDE characterizes distance maps with respect an *isotropic* metric, defined locally as f-times the euclidean metric, see [28] for a study and an overview of its numerous applications. Minimal paths w.r.t. the metric are called (minimal) geodesics, and have numerous applications in e.g. image processing [22] or motion planning. In contrast, this paper is devoted to generalized eikonal equations, characterizing distance maps with respect to anisotropic metrics, of the three following types.

- A *Riemannian metric* on a domain of $\mathbb{R}^d$ is described by a field $\mathcal{M}$ of positive definite tensors, and gives rise to the generalized eikonal equation $\|\mathrm{d}u\|_{\mathcal{M}^{-1}} = 1$. The natural metric on a surface or a manifold embedded in $\mathbb{R}^n$ is equivalent to a Riemannian metric on the parametrization domain. In image processing, anisotropic Riemannian metrics are often used to favor paths aligned with tubular structures of interest [4, 8] for segmentation. Seismic and oil prospection studies often require to estimate the arrival times of waves travelling through anisotropic, layered soil structures, which at large scales can be modeled by anisotropic Riemannian metrics, see the discussion in [30].

- A *sub-Riemannian metric* can be regarded as a degenerate Riemannian metric, which tensors have some infinite eigenvalues. Interestingly, path energies of the form $\int_0^T \alpha\sqrt{1+\kappa^2}$, depending on the path curvature κ, can be encoded into appropriate subRiemannian metrics on the product space $\mathbb{R}^d \times \mathbb{S}^{d-1}$, see [25, 12] for a numerical study with applications to image segmentation and motion planning. An alternative sub-Riemannian model is also studied in this paper, posed on $\mathbb{R}^3 \times \mathbb{S}^2$ and related to the penalization of path torsion, instead of curvature, with potential applications in vessel segmentation in the spirit of [33].

- A *Rander metric* is defined locally as the sum of a Riemannian metric $\mathcal{M}$ and of a sufficiently small co-vector field $\hat{\eta}$, see [23] and §1.3. These metrics are non-symmetric, thus define asymmetric distances, and give rise to the inhomogeneous generalization of eikonal equation $\|\mathrm{d}u - \hat{\eta}\|_{\mathcal{M}^{-1}} = 1$. The motion of a boat subject to a drift due to water currents, often called Zermelo's problem, can be encoded in a Rander metric, see §5. These metrics are also used in chapter 6 of [7] to translate region based energies, common in image segmentation tasks, into geodesic energies of the region contour. Finally, degenerate Rander metrics can encode the Euler/Mumford elastica path energy $\int_0^T \alpha(1+\kappa^2)$, where κ is the path curvature, see [6].

The objective of this paper is to design numerical schemes for computing the arrival times $u : \Omega \to \mathbb{R}$ of a front starting from the boundary of a domain Ω, and propagating at unit speed w.r.t. a given metric $\mathcal{F} : T\Omega \cong \Omega \times \mathbb{R}^d \to [0, \infty]$. In order to describe the specificity of our discretization, we briefly summarize the two classical characterizations (more mathematical background is provided after the outline). These characterisations are the eikonal PDE, and Bellman's optimality principle, which respectively read: for all $\mathbf{p} \in \Omega$

$$\mathcal{H}_{\mathbf{p}}(\mathrm{d}u(\mathbf{p})) = 1/2, \qquad\qquad u(\mathbf{p}) = \min_{\mathbf{q} \in \partial V(\mathbf{p})} u(\mathbf{q}) + d_{\mathcal{F}}(\mathbf{q}, \mathbf{p}), \tag{1}$$

where $\mathcal{H}$ denotes the Hamiltonian associated to the metric, i.e. the Legendre-Fenchel transform of the Lagrangian $\mathcal{L} := \frac{1}{2}\mathcal{F}^2$, where $V(\mathbf{p}) \subseteq \Omega$ is an arbitrary (usually chosen small) neighborhood of $\mathbf{p}$, and where $d_{\mathcal{F}}$ is the path-length distance associated to the metric $\mathcal{F}$.

The Hamiltonian approach consists in discretizing (1, left), using monotone and if possible upwind finite differences see Definition 2.1, which enable the computation of the discrete solution in a single pass. Such a discretization is proposed in this paper for Hamiltonians associated to

Riemannian and Rander metrics, generalizing results known for isotropic metrics [24]. On the other hand, the semi-Lagrangian approach consists in discretizing (1, right) by constructing suitable discrete neighborhoods $V(\mathbf{p})$, and locally approximating the distance: $d_{\mathcal{F}}(\mathbf{q},\mathbf{p}) \approx \mathcal{F}_{\mathbf{p}}(\mathbf{p}-\mathbf{q})$. The computation of the discrete solution is possible in a single pass provided each polytope $V(\mathbf{p})$, $\mathbf{p} \in \Omega$, obeys a generalized acuteness property expressed in terms of the local metric $\mathcal{F}_{\mathbf{p}}(\cdot)$, see [35]. Adaptive semi-Lagrangian schemes obeying this property were introduced by the author in [17, 18], including Fast-Marching using Lattice Basis Reduction (FM-LBR) which is the natural counterpart of the method proposed in this paper in the semi-Lagrangian setting. The main improvements brought by the FM-VR1 are the following.

- (Accuracy with second order differences) The FM-VR1 can be modified to use second order finite differences, see Remark 1.5, in contrast with most semi-Lagrangian methods, in the spirit of the Higher Accuracy Fast Marching Method (HAFMM) [28]. With a proper initialization, second order convergence rates are indeed observed, see Appendix B, both with Riemannian and Rander metrics. When first order finite differences are used, the accuracy of the FM-VR1 is close to the state of the art FM-LBR, see §B for benchmarks including comparisons with [1, 5].

- (Implementation complexity and generalization potential) Semi-Lagrangian causal discretizations of the eikonal equation require to construct local polytopes $V(\mathbf{p})$ enclosing each discretization point $\mathbf{p} \in \Omega$, and obeying a generalized acuteness geometric constraint depending on the local metric. Despite an extensive research effort [30, 1, 18, 17, 32, 15], the task is hard and only few satisfying recipes are known for anisotropic metrics. High dimensions make matters worse: for instance the 5D subRiemannian model (47) below is addressed in [12] with the FM-LBR, using 5 dimensional polytopes each having 20 vertices, 126 edges, 324 faces, 360 three dimensional facets, and 144 four dimensional facets. In contrast, the FM-VR1 numerical scheme remains simple in arbitrary dimension, and can easily be generalized by introducing e.g. asymmetric terms in the Hamiltonian [12].

- (CPU time in high dimension) In semi-Lagrangian discretizations of the eikonal equation, each elementary update of the solver requires to enumerate the facets (of all dimensions) of a complex polytope, which number grows exponentially with the dimension, see above. When using fast marching methods, performance can be improved by considering only the facets containing the last accepted point, at the expense of code simplicity. Nevertheless, these updates remain much more costly than those of the FM-VR1 in high dimensions, which amount to solve a single quadratic equation. For the 5D sub-Riemannian models described in [12] and §5, a CPU time reduction by a factor 5 was observed using the FM-VR1. This advantage however disappears in two dimensions, where the computation time of the fast marching method is dominated by the cost of maintaining a priority queue, rather than the geometric computations, see §B.

Contributions. We describe numerical schemes devoted to the computation of Riemannian, sub-Riemannian, and Rander distances, by solving the corresponding generalized eikonal equations. We prove convergence rates, based on the doubling of variables technique, see chapter [13] 10 of [31], which applies rather directly in the Riemannian case but requires non-trivial adaptations in the sub-Riemannian and Rander cases. In the Riemannian and sub-Riemannian cases, our scheme can be numerically solved via a generalized Fast Marching Method (FMM), with time complexity $\mathcal{O}(d^2 N \ln N)$ where d is the domain dimension and N is the number of discretization points. Adaptive Gauss-Siedel iteration [5] is used in the case of Rander metrics. Numerical experiments illustrate the efficiency of our numerical schemes, and their potential

applications in image segmentation and motion planning. Second order convergence rates are obtained, in the L^1 norm, when using second order finite differences.

Outline. The rest of this introduction is devoted to general notations, to the description of Voronoi's first reduction, and of elements of optimal control. The impatient reader may however jump to §1.1, §1.2 and §1.3, where the numerical schemes are described and the convergence results stated, in the Riemannian, sub-Riemannian and Rander cases respectively. Convergence proofs are provided in §2, §3 and §4 respectively. Numerical experiments are presented in §5.

General notations. Let d denote the ambient space dimension, where $2 \leq d \leq 5$ in the intended applications §5. The euclidean space and the cartesian grid are respectively denoted

$$\mathbb{E} := \mathbb{R}^d, \qquad\qquad \mathbb{L} := \mathbb{Z}^d.$$

Let $\Omega \subseteq \mathbb{E}$ be a domain, assumed throughout the paper to be bounded; additional geometrical assumptions are required in some results. For any grid scale $h > 0$ denote

$$\Omega_h := \Omega \cap h\mathbb{L} \qquad\qquad \partial\Omega_h := (\mathbb{E} \setminus \Omega) \cap h\mathbb{L}.$$

Points are denoted $\mathbf{p} \in \Omega$, vectors $\dot{\mathbf{p}} \in \mathbb{E}$, and co-vectors $\hat{\mathbf{p}} \in \mathbb{E}^*$. A special convention applies to the symbol γ, which is reserved for paths within $\overline{\Omega}$ and for which $\dot\gamma(t) := \frac{d}{dt}\gamma(t)$ denotes time derivation. We denote by $\|\dot{\mathbf{p}}\|$ the euclidean norm, by $(\dot{\mathbf{p}} \cdot \dot{\mathbf{q}})$ the scalar product and by $\langle \hat{\mathbf{p}}, \dot{\mathbf{q}} \rangle$ the duality bracket of vectors $\dot{\mathbf{p}}, \dot{\mathbf{q}} \in \mathbb{E}$, $\hat{\mathbf{p}} \in \mathbb{E}^*$. Denote by $\mathrm{GL}(\mathbb{E}) \subseteq \mathrm{L}(\mathbb{E}, \mathbb{E})$ the group of invertible linear transformations, and by $\mathrm{GL}(\mathbb{L}) \subseteq \mathrm{GL}(\mathbb{E})$ the subgroup of those which leave the cartesian grid $\mathbb{L}$ invariant - i.e. their matrix has integer coefficients and unit determinant. Denote by $\mathrm{S}(\mathbb{E}) \subseteq \mathrm{L}(\mathbb{E}, \mathbb{E}^*)$ the space of symmetric linear maps, by $\mathrm{S}^+(\mathbb{E})$ the subset of semi-definite ones, and by $\mathrm{S}^{++}(\mathbb{E})$ the positive definite ones. We adopt the notations

$$\|\dot{\mathbf{p}}\|_M := \sqrt{\langle M\dot{\mathbf{p}}, \dot{\mathbf{p}} \rangle}, \qquad\qquad \hat{\mathbf{p}} \otimes \hat{\mathbf{p}} \in \mathrm{S}^+(\mathbb{E}),$$

for the norm of $\dot{\mathbf{p}} \in \mathbb{E}$ induced by $M \in \mathrm{S}^{++}(\mathbb{E})$, and for the self outer product of $\hat{\mathbf{p}} \in \mathbb{E}^*$.

Voronoi's first reduction of quadratic forms. Following strategies dating back to Lagrange [16], Voronoi's intention was to classify the equivalence classes of positive quadratic forms, i.e. elements of $\mathrm{S}^{++}(\mathbb{E})$, under the action of the group $\mathrm{GL}(\mathbb{L})$, by attaching to them objects invariant under this action. Voronoi's first construction [26] consists of a convex set $\mathcal{P} \subseteq \mathrm{S}^{++}(\mathbb{E})$, and for each $D \in \mathrm{S}^{++}(\mathbb{E}^*)$ of a linear programming problem $\mathcal{L}(D)$:

$$\mathcal{P} := \{M \in \mathrm{S}^{++}(\mathbb{E});\, \forall \dot{\mathbf{e}} \in \mathbb{L} \setminus \{0\},\, \|\dot{\mathbf{e}}\|_M \geq 1\}, \qquad\qquad \mathcal{L}(D) := \inf_{M \in \mathcal{P}} \mathrm{Tr}(MD).$$

Introducing the duality bracket $\langle\!\langle M, D \rangle\!\rangle := \mathrm{Tr}(MD)$ between $\mathrm{S}(\mathbb{E})$ and $\mathrm{S}(\mathbb{E}^*)$, and observing that $\|\dot{\mathbf{e}}\|_M^2 = \langle\!\langle M, \dot{\mathbf{e}} \otimes \dot{\mathbf{e}} \rangle\!\rangle$, one can rephrase Voronoi's optimization problem $\mathcal{L}(D)$ as follows

$$\text{minimize } \langle\!\langle M, D \rangle\!\rangle \;\text{ subject to }\; \langle\!\langle M, \dot{\mathbf{e}} \otimes \dot{\mathbf{e}} \rangle\!\rangle \geq 1 \text{ for all } \dot{\mathbf{e}} \in \mathbb{L} \setminus \{0\}. \tag{2}$$

Theorem (Voronoi, see [26])**.** *The set $\mathcal{P} \subseteq \mathrm{S}(E)$ is a convex polytope, with a finite number of equivalence classes of vertices under the action of $\mathrm{GL}(\mathbb{L})$. The linear problem $\mathcal{L}(D)$ is feasible, in the sense that the set of minimizers is non-empty and compact, for any $D \in \mathrm{S}^{++}(\mathbb{E}^*)$.*

The vertices of the polytope $\mathcal{P}$ are called perfect quadratic forms, and are related to the densest periodic sphere packings. They are known in dimension $d \leq 6$, together with the connectivity

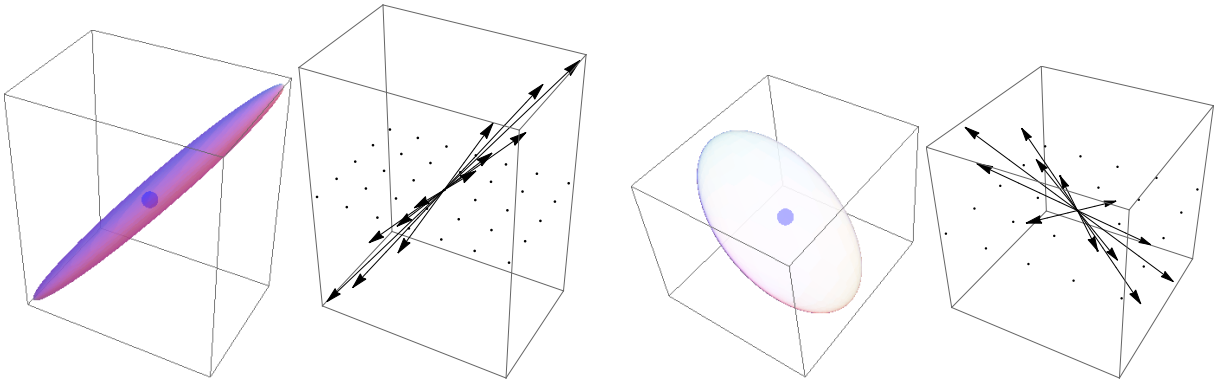

Figure 1: Ellipsoid $\{\|\dot{\mathbf{p}}\|_M \leq 1\}$, and offsets appearing in the decomposition (3) of $D := M^{-1}$, for some $M \in \mathrm{S}^{++}(\mathbb{R}^3)$ of eigenvalues $1, 10^2, 10^2$ (needle-like) and $1, 1, 10^2$ (plate-like) respectively.

of the facets of $\mathcal{P}$ see [9], which allows in principle to implement the simplex algorithm for efficiently solving (2), despite the infinite number of linear constraints. In dimension $d \in \{2, 3\}$, which is sufficient for the applications considered in this paper §5, the simplex algorithm takes a particularly simple form, because the polytope $\mathcal{P}$ only has a single equivalence class of vertices under $\mathrm{GL}(\mathbb{L})$, and it is referred to as Selling's algorithm [27, 10].

Proposition 1.1. *The Kuhn-Tucker optimality conditions for the linear optimization problem $\mathcal{L}(D)$, $D \in \mathrm{S}^{++}(\mathbb{E}^*)$, can be written as follows: there exists $(\rho_i, \dot{\mathbf{e}}_i)_{i=1}^{d'} \in (\mathbb{R}_+ \times \mathbb{L})^{d'}$, where $d' := d(d+1)/2$, such that*

$$D = \sum_{1 \leq i \leq d'} \rho_i \, \dot{\mathbf{e}}_i \otimes \dot{\mathbf{e}}_i. \tag{3}$$

Furthermore there exists $C = C(d)$ such that for any $1 \leq i \leq d'$

$$\|\dot{\mathbf{e}}_i\| \leq C \, \mathrm{Cond}(D)^{d-1}, \qquad \text{where } \mathrm{Cond}(D) := \sqrt{\|D\|\|D^{-1}\|}. \tag{4}$$

Proof. The first point (3) follows from the feasibility of the linear program $\mathcal{L}(D)$, and its formulation (2) . The number $d(d+1)/2$ of contributions in this decomposition is the number of independent entries in a $d \times d$ symmetric matrix.

For proving the second point, the euclidean space $\mathbb{E}$ is identified with its dual, which gives meaning to the trace $\mathrm{Tr}(M)$ and determinant $\det(M)$ of any $M \in \mathrm{S}^{++}(\mathbb{E})$. Denote by $(M_k)_{k=1}^K$ a representative of each equivalence class of vertices of $\mathcal{P}$ under the action of of $\mathrm{GL}(\mathbb{L})$, see Theorem 1. Let $D \in \mathrm{S}^{++}(\mathbb{E}^*)$ be arbitrary, and let M be the minimizer of $\mathcal{L}(D)$. Then $M = A^{\mathrm{T}} M_k A$ for some $1 \leq k \leq K$ and some $A \in \mathrm{GL}(\mathbb{L})$. Thus $\det(M) \geq \min_{k=1}^K \det(M_k) =: c_\Delta > 0$. On the other hand, $\mathrm{Tr}(M)\|D^{-1}\|^{-1} \leq \mathrm{Tr}(MD) \leq \mathrm{Tr}(\mathrm{Id}\, D) \leq d\|D\|$, by sub-optimality of $\mathrm{Id} \in \mathcal{P}$, hence $\mathrm{Tr}(M) \leq d\,\mathrm{Cond}(D)^2$. For any $1 \leq i \leq d'$ one has $\|\dot{\mathbf{e}}_i\|_M = 1$, since the corresponding constraint of the linear problem $\mathcal{L}(D)$ is active, hence as announced

$$\|\dot{\mathbf{e}}_i\|^2 \leq \|M^{-1}\|\|\dot{\mathbf{e}}_i\|_M^2 = \|M^{-1}\| \leq \frac{\|M\|^{d-1}}{\det(M)} \leq \frac{\mathrm{Tr}(M)^{d-1}}{c_\Delta} \leq \frac{(d\,\mathrm{Cond}(D)^2)^{d-1}}{c_\Delta}. \qquad \square$$

The formula (3) is reminiscent of the decomposition $D = \sum_{i=1}^d \lambda_i \dot{\mathbf{v}}_i \otimes \dot{\mathbf{v}}_i$ in terms of the normalized eigenvectors $\dot{\mathbf{v}}_i$ and associated eigenvalues λ_i, $1 \leq i \leq d$, of the matrix D. The number of terms d and d' in the sum differ however, and most importantly the vectors $\dot{\mathbf{e}}_i \in \mathbb{L}$ have integer coefficients and can thus be used as offsets in a finite difference scheme on a grid, see

Theorem 1.3 below, in contrast with the eigenvectors $\dot{\mathbf{v}}_i \in \mathbb{S}^{d-1}$ in general. In dimension $d \leq 3$, the decomposition (3) associated with Voronoi's first reduction can equivalently be obtained using the concept of obtuse superbase of a lattice [10]. This approach is used in [14] to design numerical schemes for anisotropic diffusion, and in [3] for Monge-Ampere equations. See [19] for an analysis finer than (4) in the the special case $d = 2$, including average case estimates upon random rotations of the tensor D.

Elements of optimal control. We refer to [2] for an overview of optimal control theory and its PDE formulations, and only introduce here the notations and definitions required for our purposes. Let $\mathfrak{C}(\mathbb{E})$ be the collection of compact and convex subsets of $\mathbb{E}$ containing the origin, equipped with the Hausdorff distance. Denote $\mathrm{Lip}(X, Y)$ the class of Lipschitz maps, with arbitrary Lipschitz constant, from a metric space X to a metric space Y.

Definition 1.2. *A family of controls is an element $\mathcal{B}$ of $\mathfrak{B} := C^0(\overline{\Omega}, \mathfrak{C}(\mathbb{E}))$, which continuously associates to each point $\mathbf{p} \in \overline{\Omega}$ a control set $\mathcal{B}(\mathbf{p})$. A path $\gamma \in \mathrm{Lip}([0, T], \overline{\Omega})$, where $T \geq 0$, is said $\mathcal{B}$-controllable iff for almost every $t \in [0, T]$*

$$\dot{\gamma}(t) \in \mathcal{B}(\gamma(t)), \qquad \text{where } \dot{\gamma}(t) := \frac{d}{dt}\gamma(t). \tag{5}$$

The minimal control time from $\mathbf{p} \in \overline{\Omega}$ to $\mathbf{q} \in \overline{\Omega}$, is defined as

$$T_{\mathcal{B}}(\mathbf{p}, \mathbf{q}) := \inf\{T \geq 0;\ \exists \gamma \in \mathrm{Lip}([0, T], \overline{\Omega}),\ \mathcal{B}\text{-controllable}, \gamma(0) = \mathbf{p}, \gamma(T) = \mathbf{q}\}. \tag{6}$$

The control sets corresponding to Riemannian, sub-Riemannian and Rander geometry are respectively ellipsoids, degenerate ellipsoids (with empty interior), and ellipsoids centered off the origin, see Figure 2. One easily shows that a minimal path from $\mathbf{p}$ to $\mathbf{q}$ exists as soon as $T_{\mathcal{B}}(\mathbf{p}, \mathbf{q}) < \infty$, using Arzela-Ascoli's compactness theorem and the fact that Ω is bounded. See [6, 12] for details, as well as related arguments such as the convergence of the control times and minimal paths associated to a converging family of controls under suitable assumptions. The framework of a local metric defined on the tangent space $\mathcal{F} : \overline{\Omega} \times \mathbb{E} \to [0, \infty]$ is often more convenient: given controls $\mathcal{B} \in \mathfrak{B}$, define for all $\mathbf{p} \in \overline{\Omega}$, $\dot{\mathbf{p}} \in \mathbb{E}$, and any path $\gamma \in \mathrm{Lip}([0, 1], \overline{\Omega})$

$$\mathcal{F}_{\mathbf{p}}(\dot{\mathbf{p}}) := \inf\{\lambda > 0; \dot{\mathbf{p}}/\lambda \in \mathcal{B}(\mathbf{p})\}, \qquad \mathrm{Length}_{\mathcal{F}}(\gamma) := \int_0^1 \mathcal{F}_{\gamma(t)}(\dot{\gamma}(t))dt.$$

Note that these quantities can be infinite if the control sets have empty interior, as in the sub-Riemannian case, or asymmetric if the control sets are not centered on the origin, as in the Rander case, see Figure 2 and §1.2, 1.3. Conversely, the metric $\mathcal{F}$ uniquely determines the control sets $\mathcal{B}(\mathbf{p}) = \{\dot{\mathbf{p}} \in \mathbb{E}; \mathcal{F}_{\mathbf{p}}(\dot{\mathbf{p}}) \leq 1\}$, and by time reparametrization the control time $T_{\mathcal{B}}(\mathbf{p}, \mathbf{q})$ from $\mathbf{p}$ to $\mathbf{q} \in \Omega$ is shown equal to the (pseudo-)distance

$$d_{\mathcal{F}}(\mathbf{p}, \mathbf{q}) := \inf\{\mathrm{Length}_{\mathcal{F}}(\gamma);\ \gamma \in \mathrm{Lip}([0, 1], \overline{\Omega}), \gamma(0) = \mathbf{p}, \gamma(1) = \mathbf{q}\}. \tag{7}$$

This paper is concerned with the exit time optimal control problem, which value function is defined for all $\mathbf{p} \in \overline{\Omega}$ by

$$u(\mathbf{q}) := \inf_{\mathbf{p} \in \partial\Omega} T_{\mathcal{B}}(\mathbf{p}, \mathbf{q}) \qquad \left(= \inf_{\mathbf{p} \in \partial\Omega} d_{\mathcal{F}}(\mathbf{p}, \mathbf{q}) \right). \tag{8}$$

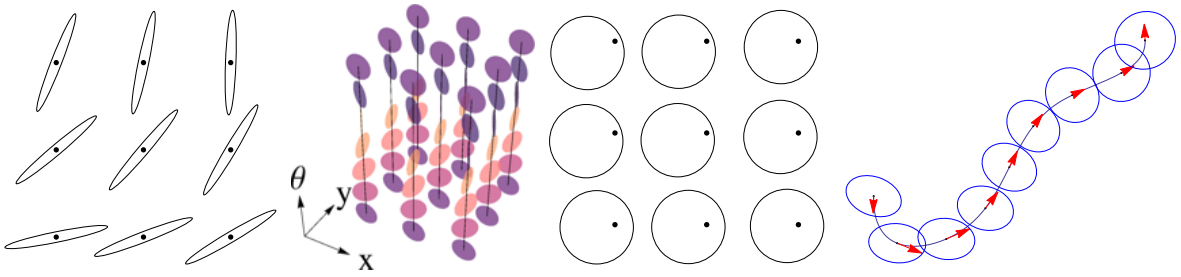

Figure 2: From left to right. Examples of control sets for a (i) Riemannian, (ii) sub-Riemannian, (iii) Rander metric. (iv) An admissible path, with tangents shown in red, w.r.t to some controls.

The numerical computation of the function u is the main topic of this paper. Under suitable assumptions [2], the function u is the unique viscosity solution to the following HJB PDE involving the dual metric $\mathcal{F}^* : \overline{\Omega} \times \mathbb{E}^* \to \mathbb{R}_+$: for all $\mathbf{p} \in \Omega$

$$\mathcal{F}^*_{\mathbf{p}}(\mathrm{d}u(\mathbf{p})) = 1, \qquad \text{where } \mathcal{F}^*_{\mathbf{p}}(\hat{\mathbf{p}}) := \sup_{\dot{\mathbf{p}} \neq 0} \frac{\langle \hat{\mathbf{p}}, \dot{\mathbf{p}} \rangle}{\mathcal{F}_{\mathbf{p}}(\dot{\mathbf{p}})}, \tag{9}$$

and $u(\mathbf{p}) = 0$ for all $\mathbf{p} \in \partial\Omega$. The formulations (9, left) and (1, left) of the eikonal PDE are equivalent, since the Hamiltonian is $\mathcal{H} = \frac{1}{2}(\mathcal{F}^*)^2$. Once u is known, the shortest path from $\partial\Omega$ to $\mathbf{p} \in \Omega$ can be extracted by solving *backwards in time* the Ordinary Differential Equation (ODE)

$$\dot{\gamma}(t) := \mathrm{d}\mathcal{F}^*_{\gamma(t)}(\mathrm{d}u(\gamma(t))), \tag{10}$$

with final condition $\gamma(T) = \mathbf{p}$ where $T = u(\mathbf{p})$, see e.g. appendix C in [12]. The differential $\mathrm{d}\mathcal{F}_{\mathbf{p}}(\hat{\mathbf{p}}) \in (\mathbb{E}^*)^* \cong \mathbb{E}$ appearing in (10) is meant w.r.t. the second variable $\hat{\mathbf{p}}$.

1.1 Riemannian metrics

A Riemannian metric on the bounded domain $\Omega \subseteq \mathbb{E}$, is described via a field of positive definite tensors $\mathcal{M} \in C^0(\overline{\Omega}, \mathrm{S}^{++}(\mathbb{E}))$. The metric function $\mathcal{F} : \overline{\Omega} \times \mathbb{E} \to \mathbb{R}_+$ has the expression

$$\mathcal{F}_{\mathbf{p}}(\dot{\mathbf{p}}) := \|\dot{\mathbf{p}}\|_{\mathcal{M}(\mathbf{p})}. \tag{11}$$

Our objective is to compute the Riemannian distance $u : \overline{\Omega} \to \mathbb{R}$ to the boundary of Ω, see (8), which is known to be the unique viscosity solution [11] to the Riemannian eikonal equation: for all $\mathbf{p} \in \Omega$

$$\|\mathrm{d}u(\mathbf{p})\|_{\mathcal{D}(\mathbf{p})} = 1 \qquad \text{where } \mathcal{D}(\mathbf{p}) := \mathcal{M}(\mathbf{p})^{-1}, \tag{12}$$

and $u(\mathbf{p}) = 0$ for all $\mathbf{p} \in \partial\Omega$. Indeed, the dual to the Riemannian metric (11) reads $\mathcal{F}^*_{\mathbf{p}}(\hat{\mathbf{p}}) = \|\hat{\mathbf{p}}\|_{\mathcal{D}(\mathbf{p})}$. For each $\mathbf{p} \in \overline{\Omega}$, let $(\rho_i(\mathbf{p}), \dot{\mathbf{e}}_i(\mathbf{p}))_{i=1}^{d'} \in (\mathbb{R}_+ \times \mathbb{L})^{d'}$ be weights and offsets such that

$$\mathcal{D}(\mathbf{p}) = \sum_{1 \leq i \leq d'} \rho_i(\mathbf{p})\, \dot{\mathbf{e}}_i(\mathbf{p}) \otimes \dot{\mathbf{e}}_i(\mathbf{p}). \tag{13}$$

In this paper, we advocate the use of Voronoi's first reduction of quadratic forms for obtaining the decomposition (13), see Proposition 1.1. Our convergence results however only require to control the maximal stencil radius

$$r_* := \max\{\|\dot{\mathbf{e}}_i(\mathbf{p})\|;\, \mathbf{p} \in \overline{\Omega}, 1 \leq i \leq d'\}. \tag{14}$$

If Proposition 1.1 is used for stencil construction, then r_* is by (4) bounded in terms of the maximal condition number of the metric, and $d' = d(d+1)/2$. For the sake of readability, we omit in the rest of the paper to write the dependence of the offset $\dot{\mathbf{e}}_i = \dot{\mathbf{e}}_i(\mathbf{p})$ on the point $\mathbf{p} \in \overline{\Omega}$.

Theorem 1.3. *Let $\mathcal{M} \in C^0(\overline{\Omega}, \mathrm{S}^{++}(\mathbb{E}))$ be a Riemannian metric, and for all $\mathbf{p} \in \overline{\Omega}$ let $\mathcal{D}(\mathbf{p}) := \mathcal{M}(\mathbf{p})^{-1}$ and $(\rho_i(\mathbf{p}), \dot{\mathbf{e}}_i(\mathbf{p}))_{i=1}^{d'}$ be as in (13). Then for any $h > 0$ there exists a unique solution $U_h : h\mathbb{L} \to \mathbb{R}$ to the following discrete problem: for all $\mathbf{p} \in \Omega_h$*

$$h^{-2} \sum_{1 \leq i \leq d'} \rho_i(\mathbf{p}) \max\{0,\, U_h(\mathbf{p}) - U_h(\mathbf{p} + h\dot{\mathbf{e}}_i),\, U_h(\mathbf{p}) - U_h(\mathbf{p} - h\dot{\mathbf{e}}_i)\}^2 = 1 \tag{15}$$

and $U_h(\mathbf{p}) = 0$ for all $\mathbf{p} \in \partial\Omega_h$. The solution U_h can be computed via the fast-marching algorithm with complexity $\mathcal{O}(d' N_h \ln N_h)$, where $N_h = \#(\Omega_h)$. If in addition the domain Ω satisfies an exterior cone condition, and if $\mathcal{M} \in \mathrm{Lip}(\overline{\Omega}, \mathrm{S}^{++}(\mathbb{E}))$, then for some constant $C = C(\mathcal{M}, \Omega)$ one has for all $h > 0$

$$\max_{\mathbf{p} \in \Omega_h} |U_h(\mathbf{p}) - u(\mathbf{p})| \leq C\sqrt{r_* h}. \tag{16}$$

The estimate (16) outlines the importance of the stencil radius r_*, since it determines the *effective* scale $r_* h$ of the discretization and thus the accuracy of the numerical method. A similar convergence rate is obtained in [31] for the Ordered Upwind Method [30], a semi-Lagrangian solver of anisotropic eikonal equations. In [19], the construction of Proposition 1.1 is shown to be optimal in terms of stencil radius, in dimension $d = 2$. Note that the dependency of the constant $C = C(\Omega, \mathcal{M})$ in (16) with respect to the metric $\mathcal{M}$ is not explicited in Theorem 1.3. This point is analyzed in detail in the next sub-section, where we consider a family of increasingly anisotropic Riemannian metrics converging to a degenerate sub-Riemannian model.

The minimal geodesics from $\partial\Omega$ obey, in view of (10) and of the dual metric expression $\mathcal{F}^*_{\mathbf{p}}(\hat{\mathbf{p}}) = \|\hat{\mathbf{p}}\|_{\mathcal{D}(\mathbf{p})}$, the (ODE)

$$\dot{\gamma}(t) = \mathcal{D}(\gamma(t))\mathrm{d}u(\gamma(t)).$$

The direction of these geodesics can be directly extracted from the numerical scheme, thanks to the following proposition which generalises a similar result in the isotropic case in [24].

Proposition 1.4. *For each $\mathbf{p} \in \Omega_h$ one has the formally consistent approximation*

$$\mathcal{D}(\mathbf{p})\mathrm{d}u(\mathbf{p}) \approx h^{-1} \sum_{1 \leq i \leq d'} \varepsilon_i \rho_i(\mathbf{p}) \max\{0,\, U_h(\mathbf{p}) - U_h(\mathbf{p} + h\dot{\mathbf{e}}_i),\, U_h(\mathbf{p}) - U_h(\mathbf{p} - h\dot{\mathbf{e}}_i)\}\dot{\mathbf{e}}_i, \tag{17}$$

where for each $1 \leq i \leq d'$ one defines $\varepsilon_i = 0$ (resp. $\varepsilon_i = -1$, resp. $\varepsilon_i = 1$) if the i-th maximum is 0 (resp. $U_h(\mathbf{p}) - U_h(\mathbf{p} + h\dot{\mathbf{e}}_i)$, resp. $U_h(\mathbf{p}) - U_h(\mathbf{p} - h\dot{\mathbf{e}}_i)$).

Proof. By consistent we mean that the formula (17) is exact if $u = U_h$ is a linear function, say $U(\mathbf{p}) = \langle \hat{\eta}, \mathbf{p} - \mathbf{p}_0 \rangle$. In that case the r.h.s of (17) becomes by (13)

$$h^{-1} \sum_{1 \leq i \leq d'} \varepsilon_i \rho_i(\mathbf{p}) |\langle \hat{\eta}, h\dot{\mathbf{e}}_i \rangle| \dot{\mathbf{e}}_i = \sum_{1 \leq i \leq d'} \rho_i(\mathbf{p}) \langle \hat{\eta}, \dot{\mathbf{e}}_i \rangle \dot{\mathbf{e}}_i = \mathcal{D}(\mathbf{p})\hat{\eta} = \mathcal{D}(\mathbf{p})\mathrm{d}u(\mathbf{p}). \qquad \square$$

Remark 1.5 (Second order scheme)**.** *The Discretization (15) is based on the first order approximation $\langle \mathrm{d}U(\mathbf{p}), \dot{\mathbf{e}} \rangle = \frac{1}{h}(U(\mathbf{p} + h\dot{\mathbf{e}}) - U(\mathbf{p})) + \mathcal{O}(h)$, for smooth U, $\dot{\mathbf{e}} \in \mathbb{R}$, and small $h > 0$. In the spirit of the HAFMM [28] we experiment numerically in §5 the use when possible of*

$$\langle \mathrm{d}U(\mathbf{p}), \dot{\mathbf{e}} \rangle = \frac{1}{h}(U(\mathbf{p} + h\dot{\mathbf{e}}) - U(\mathbf{p})) - \frac{1}{2h}(U(\mathbf{p}) - 2U(\mathbf{p} + h\dot{\mathbf{e}}) + U(\mathbf{p} + 2h\dot{\mathbf{e}})) + \mathcal{O}(h^2).$$

Second order accuracy is indeed observed, provided the boundary conditions are smooth.

1.2 Sub-Riemannian metrics

We introduce a numerical scheme for the computation of sub-Riemannian distances and geodesics, based on solving by fast marching the eikonal equations associated to a sequence of increasingly anisotropic approximate Riemannian metrics, in the spirit of [25]. More precisely our results apply to the slightly more general class of pre-Riemannian models.

Definition 1.6. *A pre-Riemannian model on Ω is a finite family of vector fields $\dot\omega_1, \cdots, \dot\omega_n \in \mathrm{Lip}(\overline{\Omega}, \mathbb{E})$. The control sets $\mathcal{B} \in \mathrm{Lip}(\overline{\Omega}, \mathfrak{C}(\mathbb{E}))$, and the semi-definite tensor field $\mathcal{D} \in \mathrm{Lip}(\overline{\Omega}, \mathrm{S}^+(\mathbb{E}^*))$, for this model are defined for all $\mathbf{p} \in \overline{\Omega}$ by*

$$\mathcal{B}(\mathbf{p}) := \{ \sum_{1\le i\le n} \alpha_i \dot\omega_i(\mathbf{p});\ \alpha \in \mathbb{R}^n,\ \sum_{1\le i\le n} \alpha_i^2 \le 1\}, \qquad \mathcal{D}(\mathbf{p}) := \sum_{1\le i\le n} \dot\omega_i(\mathbf{p}) \otimes \dot\omega_i(\mathbf{p}).$$

A sub-Riemannian model [20] of step $k \ge 0$ is a pre-Riemannian model with the additional properties that the vector fields are smooth and that, together with their iterated commutators up to depth k, they span the tangent space $\mathbb{E}$ at each point $\mathbf{p} \in \overline{\Omega}$. The minimal control time $T_{\mathcal{B}}(\mathbf{p}, \mathbf{q})$ for a sub-Riemannian model is called the Carnot-Theodory distance, and by Chow's theorem it obeys $T_{\mathcal{B}}(\mathbf{p}, \mathbf{q}) \le C|\mathbf{p} - \mathbf{q}|^{\frac{1}{k}}$. The distance u to $\partial\Omega$ is the unique viscosity solution to the sub-Riemannian eikonal equation: $\|\mathrm{d}u(\mathbf{p})\|_{\mathcal{D}(\mathbf{p})} = 1$ for all $\mathbf{p} \in \Omega$, and $u = 0$ on $\partial\Omega$.

For better or worse, we do not use any techniques or results from sub-Riemannian geometry in this paper, but stick instead to the simpler pre-Riemannian concept. We do however make a further assumption.

Assumption 1.7. *We fix a pre-Riemannian model $(\dot\omega_i)_{i=1}^n$, and assume that the exit time value function u, defined in (8), is bounded on Ω. We further assume that the domain admits outward normals $\dot{\mathbf{n}}(\mathbf{p})$ with Lipschitz regularity on $\partial\Omega$, and that for each $\mathbf{p} \in \partial\Omega$ there exists $1 \le i \le n$ such that $\dot{\mathbf{n}}(\mathbf{p}) \cdot \dot\omega_i(\mathbf{p}) \ne 0$.*

The finiteness of u on Ω, a *global controllability* assumption, is obviously required if one intends to prove convergence rates of discrete approximations of u. The second assumption, is related to *short time local controllability at the boundary* [2], and implies in particular the Lipschitz regularity of u, via Gronwall's lemma see §3.1.

Definition 1.8. *A completion of a pre-Riemannian model $(\dot\omega_i)_{i=1}^n$ is a second finite family of vector fields $\dot\omega_1^*, \ldots, \dot\omega_{n^*}^* \in \mathrm{Lip}(\overline{\Omega}, \mathbb{E})$, such that $\dot\omega_1(\mathbf{p}), \cdots, \omega_n(\mathbf{p}), \dot\omega_1^*(\mathbf{p}), \cdots, \dot\omega_{n^*}^*(\mathbf{p})$ spans $\mathbb{E}$ for each $\mathbf{p} \in \overline{\Omega}$.*

For each $0 < \varepsilon \le 1$ the augmented pre-Riemannian model $(\omega_1, \cdots, \omega_n, \varepsilon\omega_1^*, \cdots, \varepsilon\omega_{n^*}^*)$ is equivalent (i.e. has the same control sets) to the Riemannian model of metric $\mathcal{M}_\varepsilon := \mathcal{D}_\varepsilon^{-1}$, where

$$\mathcal{D}_\varepsilon = \mathcal{D} + \varepsilon^2 \mathcal{D}^*, \qquad \text{with } \mathcal{D}^* := \sum_{1\le i\le n^*} \dot\omega_i^* \otimes \dot\omega_i^*. \tag{18}$$

In order to solve numerically the pre-Riemannian exit time problem, our strategy is to apply the scheme of Theorem 1.3 to the positive definite (but strongly anisotropic) Riemannian metric $\mathcal{M}_\varepsilon$, for small $\varepsilon > 0$. Convergence towards the pre-Riemannian exit times $u : \Omega \to \mathbb{R}$ is established in the next theorem, when the relaxation parameter ε and grid scale h tend to 0 suitably.

Theorem 1.9. *Consider a pre-Riemannian model $\dot\omega_1, \cdots, \dot\omega_n \in \mathrm{Lip}(\overline\Omega, \mathbb{E})$ obeying Assumption 1.7, and a completion $\dot\omega_1^*, \cdots, \dot\omega_n^*$. For each $0 < \varepsilon \leq 1$ let u_ε distance to $\partial\Omega$ for the Riemannian metric $\mathcal{M}_\varepsilon$, and let $U_{h,\varepsilon}$ be the discrete solution of (15) with scale $h > 0$. Then*

$$\max_{\overline\Omega} |u - u_\varepsilon| \leq C\varepsilon, \qquad\qquad \max_{\Omega_h} |u_\varepsilon - U_{h,\varepsilon}| \leq C'\sqrt{r_\varepsilon h}, \tag{19}$$

where r_ε denotes the maximal stencil radius for $\mathcal{M}_\varepsilon$, see (14), and where C, C' only depend on $\Omega, (\dot\omega_i)_{i=1}^n, (\dot\omega_i^*)_{i=1}^{n^*}$. In particular $U_{h,\varepsilon} \to u$ uniformly as $\varepsilon \to 0$ and $h\, r_\varepsilon \to 0$.

By construction the condition number of the tensors $\mathcal{M}_\varepsilon$ is $\mathcal{O}(\varepsilon^{-1})$, hence $r_\varepsilon \leq C\varepsilon^{-(d-1)}$ if Proposition 1.1 is used for the stencil construction. The convergence rate $\max_{\Omega_h} |U_{h,\varepsilon} - u| \leq Ch^{\frac{1}{d+1}}$ is thus ensured by choosing $\varepsilon = h^{\frac{1}{d+1}}$.

1.3 Rander geometry

Rander metrics are asymmetric metrics, defined as the sum of a symmetric Riemannian part and of an anti-symmetric linear part [23]. A Rander metric is thus described by a tensor field $\mathcal{M} \in C^0(\overline\Omega, \mathrm{S}^{++}(\mathbb{E}))$, and a sufficiently small co-vector field $\hat\eta \in C^0(\overline\Omega, \mathbb{E}^*)$

$$\mathcal{F}_{\mathbf{p}}(\dot{\mathbf{p}}) := \|\dot{\mathbf{p}}\|_{\mathcal{M}(\mathbf{p})} + \langle \hat\eta(\mathbf{p}), \dot{\mathbf{p}}\rangle, \qquad\qquad \text{where } \|\hat\eta(\mathbf{p})\|_{\mathcal{M}(\mathbf{p})^{-1}} < 1. \tag{20}$$

The smallness constraint (20, right) ensures the positivity of the asymmetric norm $\mathcal{F}_{\mathbf{p}}(\cdot)$. The distance induced by a Rander metric is oriented: $d_{\mathcal{F}}(\mathbf{p}, \mathbf{q}) \neq d_{\mathcal{F}}(\mathbf{q}, \mathbf{p})$ in general.

Proposition 1.10. *The distance u to $\partial\Omega$, see (8), is the unique the viscosity solution to the inhomogeneous static first order HJB PDE*

$$\|\mathrm{d}u(\mathbf{p}) - \hat\eta(\mathbf{p})\|_{\mathcal{D}(\mathbf{p})} = 1, \qquad\qquad \text{where } \mathcal{D}(\mathbf{p}) = \mathcal{M}(\mathbf{p})^{-1}, \tag{21}$$

for all $\mathbf{p} \in \Omega$, and $u = 0$ on $\partial\Omega$.

Proof. It is known that u solves the eikonal PDE $\mathcal{F}_{\mathbf{p}}^*(\mathrm{d}u(\mathbf{p})) = 1$, see (9). Now for any $\hat{\mathbf{p}} \in \mathbb{E}^*$ observe the sequence of equivalences:

$$\begin{aligned}
\mathcal{F}_{\mathbf{p}}^*(\hat{\mathbf{p}}) = 1 \;&\Leftrightarrow\; \exists \dot{\mathbf{p}} \in \mathbb{E} \setminus \{0\}, \hat{\mathbf{p}} = \mathrm{d}\mathcal{F}_{\mathbf{p}}(\dot{\mathbf{p}}) \\
&\Leftrightarrow\; \exists \dot{\mathbf{p}} \in \mathbb{E} \setminus \{0\}, \hat{\mathbf{p}} = \mathcal{M}(\mathbf{p})\dot{\mathbf{p}}/\|\dot{\mathbf{p}}\|_{\mathcal{M}(\mathbf{p})} + \hat\eta(\mathbf{p}) \\
&\Leftrightarrow\; \|\hat{\mathbf{p}} - \hat\eta(\mathbf{p})\|_{\mathcal{D}(\mathbf{p})} = 1.
\end{aligned}$$

The first equivalence follows from convex duality $\mathcal{F}^*(\mathrm{d}\mathcal{F}(\dot{\mathbf{p}})) = 1$, $\forall \dot{\mathbf{p}} \in \mathbb{E}$, and the second one from the explicit expression (20) of $\mathcal{F}$. □

Theorem 1.11. *Let $(\mathcal{M}, \hat\eta)$ be a Rander metric, and for all $\mathbf{p} \in \overline\Omega$ let $\mathcal{D}(\mathbf{p}) := \mathcal{M}(\mathbf{p})^{-1}$ and $(\rho_i(\mathbf{p}), \dot{\mathbf{e}}_i(\mathbf{p}))_{i=1}^{d'}$ be as in (13). Then for any $h > 0$ there exists a unique solution to $U_h : h\mathbb{L} \to \mathbb{R}$ to the discrete problem: for all $\mathbf{p} \in \Omega_h$*

$$\sum \lambda_i(\mathbf{p}) \max\{0,\, U_h(\mathbf{p}) - U_h(\mathbf{p} + h\dot{\mathbf{e}}_i) + h\langle\hat\eta(\mathbf{p}), \dot{\mathbf{e}}_i\rangle,\, U_h(\mathbf{p}) - U_h(\mathbf{p} - h\dot{\mathbf{e}}_i) - h\langle\hat\eta(\mathbf{p}), \dot{\mathbf{e}}_i\rangle\}^2 = h^2, \tag{22}$$

and $U_h(\mathbf{p}) = 0$ for all $\mathbf{p} \in \partial\Omega_h$. If in addition Ω obeys an exterior cone condition, and $\mathcal{M}$ and η have Lipschitz regularity, then for some $C = C(\Omega, \mathcal{M}, \hat\eta)$ one has for all $h > 0$

$$\max_{\mathbf{p} \in \Omega_h} |U_h(\mathbf{p}) - u(\mathbf{p})| \leq C\sqrt{r_* h}.$$

The discretized PDE (22) cannot be solved using the Fast-Marching algorithm, contrary to the Riemannian case (15) and sub-Riemannian case, because the expression (22) may depend on non-causal, negative finite differences $U(\mathbf{p})-U(\mathbf{p}+\dot{\mathbf{e}})<0$ when $\langle\hat{\eta}(\mathbf{p}),\dot{\mathbf{e}}\rangle\neq 0$, see Definition 2.1. For moderate anisotropies, good results are nevertheless obtained using Adaptive Gauss Siedel Iteration (AGSI), see [5] and §5. Note that fast marching algorithm compatible with Rander metrics, semi-Lagrangian and two dimensional only, is described in [17].

The numerical scheme (22) can, similarly to the Riemannian case, be used to reconstruct the differential $\mathrm{d}u$. The proof, similar to Proposition 1.4, is left to the reader.

Proposition 1.12. *For each $\mathbf{p}\in\Omega_h$, one has the approximation, exact for linear u,*

$$\mathcal{D}(\mathbf{p})(\mathrm{d}u(\mathbf{p})-\hat{\eta}(\mathbf{p}))\approx$$
$$\sum\varepsilon_i\lambda_i(\mathbf{p})\max\{0,\,U_h(\mathbf{p})-U_h(\mathbf{p}+h\dot{\mathbf{e}}_i)+h\langle\hat{\eta}(\mathbf{p}),\dot{\mathbf{e}}_i\rangle,\,U_h(\mathbf{p})-U_h(\mathbf{p}-h\dot{\mathbf{e}}_i)-h\langle\hat{\eta}(\mathbf{p}),\dot{\mathbf{e}}_i\rangle\}\dot{\mathbf{e}}_i,$$

where $\varepsilon_i=0$ (resp. -1, resp. 1) if the i-th maximum is attained for the first term (resp. second term, resp. third term).

The dual to a Rander metric $\mathcal{F}=\mathcal{F}(\mathcal{M},\hat{\eta})$ is known to be a Rander metric as well $\mathcal{F}^*=\mathcal{F}(\mathcal{M}^*,\dot{\eta}^*)$, which tensor field $\mathcal{M}^*\in C^0(\overline{\Omega},\mathrm{S}^{++}(\mathbb{E}^*))$ and vector field $\dot{\eta}^*\in C^0(\overline{\Omega},\mathbb{E})$ have simple algebraic expressions in terms of $\mathcal{M},\hat{\eta}$, given [17]. The next proposition describes the Rander geodesic ODE, and expresses the Rander metric control sets and shifted ellipsoids, which is used in §5 for modeling motion subject to drifts [23].

Proposition 1.13. *Let $\mathcal{F}=\mathcal{F}(\mathcal{M},\hat{\eta})$, as in (20), be a Rander metric with dual $\mathcal{F}^*=\mathcal{F}(\mathcal{M}^*,\dot{\eta}^*)$. Then the geodesic ODE and the control sets read respectively with $\mathcal{D}^*:=(\mathcal{M}^*)^{-1}$*

$$\dot{\gamma}(t)=\frac{\mathcal{M}^*(\gamma(t))\mathrm{d}u(\gamma(t))}{\|\mathrm{d}u(\gamma(t))\|_{\mathcal{M}^*(\gamma(t))}}+\dot{\eta}^*(\gamma(t)),\qquad \mathcal{B}(\mathbf{p})=\{\dot{\mathbf{v}}-\dot{\eta}^*(\mathbf{p});\,\|\dot{\mathbf{v}}\|_{\mathcal{D}^*(\mathbf{p})}\leq 1\}.\tag{23}$$

Proof. The geodesic ODE (23, left) follows from (10) and the explicit expression of $\mathcal{F}^*$. The control set expression (23, right) follows from the observation, similarly to the proof of Proposition 1.10, that $\dot{\mathbf{p}}\in\partial\mathcal{B}(\mathbf{p})$ iff $\mathcal{F}_{\mathbf{p}}(\dot{\mathbf{p}})=1$ iff $\exists\hat{\mathbf{p}}\in\mathbb{E}^*\setminus\{0\}$, $\dot{\mathbf{p}}=\mathrm{d}\mathcal{F}^*(\hat{\mathbf{p}})=\mathcal{M}^*(\mathbf{p})\hat{\mathbf{p}}/\|\hat{\mathbf{p}}\|_{\mathcal{M}^*(\mathbf{p})}+\dot{\eta}^*(\mathbf{p})$. □

2 Convergence in the Riemannian case

This section is devoted to the proof of Theorem 1.3, which contains two parts: a claim of well-posedness for the system of equations discretizing the Riemannian eikonal PDE, and an error analysis as the grid scale is refined. For that purpose, two general and classical results are stated in §2.1, and later specialized in §2.2 to the model of interest.

2.1 Two general results

We present (reformulations of) two classical results. First, the existence and uniqueness of solutions to monotone schemes and the algorithmic solution to causal schemes, in the spirit of [34, 21] and under adequate assumptions, are stated in Theorem 2.2. Second, the doubling of variables argument, a strategy for numerical analysis adapted [13], is stated in Theorem 2.3.

Definition 2.1. *A (finite differences) scheme on a finite set X is a continuous map $\mathfrak{F}:X\times\mathbb{R}\times\mathbb{R}^X\to\mathbb{R}$. The scheme is said:*

- *Monotone, iff $\mathfrak{F}$ is non-decreasing w.r.t. the second and (each of the) third variables.*
- *Causal, iff $\mathfrak{F}$ only depends on the positive part of the third variable.*

To the scheme is associated a function $\mathbb{R}^X \to \mathbb{R}^X$ still (abusively) denoted by $\mathfrak{F}$, and defined by

$$(\mathfrak{F}U)(\mathbf{x}) := \mathfrak{F}(\mathbf{x}, U(\mathbf{x}), (U(\mathbf{x}) - U(\mathbf{y}))_{\mathbf{y}\in X}),$$

for all $\mathbf{x} \in X$, $U \in \mathbb{R}^X$. A discrete map $U \in \mathbb{R}^X$ is called a sub- (resp. strict sub-, resp. super-, resp. strict super-) solution of the scheme $\mathfrak{F}$ iff $\mathfrak{F}U \leq 0$ (resp. $\mathfrak{F}U < 0$, resp. $\mathfrak{F}U \geq 0$, resp. $\mathfrak{F}U > 0$) pointwise on X.

When the scheme $\mathfrak{F}$ is obvious from context, we simply speak of sub- and super-solution.

Theorem 2.2 (Solving monotone schemes)**.** *Let $\mathfrak{F}$ be a monotone scheme on a finite set X s.t.*

(i) There exists a sub-solution U^- and a super-solution U^+ to the scheme $\mathfrak{F}$.

(ii) Any super-solution to $\mathfrak{F}$ is the limit of a sequence of strict super-solutions.

Then there exists a unique solution $U \in \mathbb{R}^X$ to $\mathfrak{F}U = 0$, and it satisfies $U^- \leq U \leq U^+$. If in addition the scheme is causal, then this solution can be obtained via the Dynamic-Programming algorithm, also called Dijkstra or Fast-Marching, with complexity $\mathcal{O}(M \ln N)$ where

$$N = \#(X), \qquad M = \#(\{(x, y) \in X \times X;\ \mathfrak{F}U(x) \text{ depends on } U(y)\}). \tag{24}$$

Proof. The proof is recalled for completeness. *Proof of uniqueness, via the comparison principle.* Let U^+ be a strict super-solution, and U^- a sub-solution. Let $\mathbf{p} \in X$ be such that $U^-(\mathbf{p}) - U^+(\mathbf{p})$ is maximal, so that $U^-(\mathbf{p}) - U^-(\mathbf{q}) \geq U^+(\mathbf{p}) - U^-(\mathbf{q})$ for any $\mathbf{q} \in X$. Assuming for contradiction that $U^-(\mathbf{p}) \geq U^+(\mathbf{p})$ we obtain $0 \geq \mathfrak{F}U^-(\mathbf{p}) \geq \mathfrak{F}U^+(\mathbf{p}) > 0$ which is a contradiction, hence $U^- \leq U^+$. Next by assumption (ii) we obtain that $U^- \leq U^+$ still holds for any sub-solution U^- and any (non-strict) super solution U^+. The uniqueness of the solution to $\mathfrak{F}U = 0$ follows.

Proof of existence, by the min-max construction. Consider $U : X \to \mathbb{R}$ defined by $U(\mathbf{p}) := \sup\{\tilde{U}(\mathbf{p});\ \tilde{U} \text{ sub-solution}\}$, for all $\mathbf{p} \in X$. By the previous argument $U^- \leq U \leq U^+$. Consider an arbitrary $\mathbf{p} \in X$, and let U^* be a sub-solution such that $U(\mathbf{p}) = U^*(\mathbf{p})$, which exists by continuity of $\mathfrak{F}$. By construction $U \geq U^*$, hence $\mathfrak{F}U(\mathbf{p}) \leq \mathfrak{F}U^*(\mathbf{p}) \leq 0$, hence U is a sub-solution by arbitraryness of $\mathbf{p}$. Furthermore, assume for contradiction that there exists $\mathbf{p}_0 \in X$ such that $\mathfrak{F}U(\mathbf{p}_0) < 0$, and define $U_\varepsilon(\mathbf{p}_0) := U(\mathbf{p}_0) + \varepsilon$ and $U_\varepsilon(\mathbf{p}) := U(\mathbf{p})$ for all $\mathbf{p} \in X \setminus \{\mathbf{p}_0\}$. Then U_ε is a sub-solution for any sufficiently small $\varepsilon > 0$, by monotony and continuity of the scheme $\mathfrak{F}$, thus $U(\mathbf{p}_0) \geq U_\varepsilon(\mathbf{p}_0)$ by construction which is a contradiction. Thus $\mathfrak{F}U = 0$ identically on X and therefore U is a solution to the scheme.

We refer to [34, 24] for the description of the fast marching algorithm. □

The following result is a general strategy for proving convergence rates for discretizations of first order HJB PDEs, adapted from [13]. For completeness, the proof is presented in §C. The cartesian grid $h\mathbb{L}$ could be replaced with an arbitrary h-net of E, in other words a discrete set such that union of all balls of radius h centered at the points of this set covers $\mathbb{E}$.

Theorem 2.3 (Doubling of variables argument)**.** *Let $u : \mathbb{E} \to \mathbb{R}$ be supported on a bounded domain $\overline{\Omega}$ and C^u_{Lip}-Lipschitz, and let $U_h : h\mathbb{L} \to \mathbb{R}$ be supported on $\Omega_h := \Omega \cap h\mathbb{L}$. Given $\lambda \in [1/2, 1[$ and $\delta > 0$, define*

$$\overline{M}_{\lambda,\delta} := \sup_{(\mathbf{p},\mathbf{q})\in h\mathbb{L}\times\mathbb{E}} \lambda U_h(\mathbf{p}) - u(\mathbf{q}) - \frac{1}{2\delta}\|\mathbf{p} - \mathbf{q}\|^2, \quad \widetilde{M}_{\lambda,\delta} := \sup_{(\mathbf{p},\mathbf{q})\in h\mathbb{L}\times\mathbb{E}} \lambda u(\mathbf{q}) - U_h(\mathbf{p}) - \frac{1}{2\delta}\|\mathbf{p} - \mathbf{q}\|^2,$$

and denote by $(\overline{\mathbf{p}}, \overline{\mathbf{q}}), (\tilde{\mathbf{p}}, \tilde{\mathbf{q}}) \in (h\mathbb{L}) \times \mathbb{E}$ *the point pairs where the maxima are respectively attained. Then* $\|\mathbf{p} - \mathbf{q}\| \leq 4C^u_{\mathrm{Lip}}\delta$. *Assume furthermore that for some* C^U_{bd}, C'^U_{bd} *and* $c^U_{\mathrm{bd}} \geq 4C_{\mathrm{Lip}}\delta$ *the following holds:*

(i) None of the two maximal pairs $(\overline{\mathbf{p}}, \overline{\mathbf{q}})$ *and* $(\tilde{\mathbf{q}}, \tilde{\mathbf{q}})$ *belongs to* $\Omega_h \times \Omega$.

(ii) $|U_h(\mathbf{p})| \leq C^U_{\mathrm{bd}} d_{\partial\Omega}(\mathbf{p}) + C'^U_{\mathrm{bd}} h$, *for all* $\mathbf{p} \in \Omega_h$ *such that* $d_{\partial\Omega}(\mathbf{p}) \leq c_{\mathrm{bd}}$.

Then one has with $C_0 = 4C^u_{\mathrm{Lip}} \max\{C^u_{\mathrm{Lip}}, C^U_{\mathrm{bd}}\}$

$$\max_{\mathbf{p}\in\Omega_h} |u(\mathbf{p}) - U_h(\mathbf{p})| \leq 2\left(C_0\delta + C'^U_{\mathrm{bd}} h + (1-\lambda)\max_{\overline{\Omega}} |u|\right). \tag{25}$$

When applying Theorem 2.3, to a specific model, property (i) follows directly from the consistency of the discretization, while Property (ii) requires to establish a discrete counterpart of short-time local controllability at the boundary. Explicit expressions of the constants C^u_{Lip}, C^U_{bd}, c^U_{bd}, are provided in terms of the model parameters $\mathcal{M}, \Omega$. The constant C'^U_{bd}, also given explicitly, depends linearly on the stencil maximal radius: $C'^U_{\mathrm{bd}} = C''^U_{\mathrm{bd}} r_*$, and property (i) is shown to hold provided

$$\lambda \leq 1 - C_1\delta - C_2 r_* \frac{h}{\delta},$$

where C_1, C_2 are again explicit constants depending only on $\mathcal{M}, \Omega$. Choosing λ equal to this upper bound, and defining $\delta = \sqrt{r_* h}$, one gets the announced error estimate

$$\max_{\mathbf{p}\in\Omega_h} |u(\mathbf{p}) - U_h(\mathbf{p})| \leq 2C''^U_{\mathrm{bd}} r_* h + 2(C_0 + (C_1 + C_2)\|u\|_\infty)\sqrt{r_* h}.$$

2.2 Application to the Riemannian case

We establish Theorem 1.3, on the discretization of Riemannian exit time problems, by specializing the general results of §2.1. Consider the discretization scheme $\mathfrak{F}_h$ on the finite domain Ω_h and defined for any $U : \Omega_h \to \mathbb{R}$ and any $\mathbf{p} \in \Omega_h$ by

$$(\mathfrak{F}_h U(\mathbf{p}))^2 := h^{-2} \sum_{1\leq i\leq d'} \lambda_i(\mathbf{p}) \max\{0,\, U(\mathbf{p}) - U(\mathbf{p} + \dot{\mathbf{e}}_i),\, U(\mathbf{p}) - U(\mathbf{p} - \dot{\mathbf{e}}_i)\}^2, \tag{26}$$

where U is extended by zero on $h\mathbb{L} \setminus \Omega_h$. The next proposition implies, by Theorem 2.2, the existence and uniqueness of a solution to the equation $\mathfrak{F}_h U - 1 \equiv 0$, and the applicability of the Fast-Marching algorithm to compute it, as announced in Theorem 1.3.

Recall that r_* is the maximal stencil radius, as defined in (14). The square root of the largest eigenvalue among all tensors of a tensor field $\mathcal{M} \in C^0(\overline{\Omega}, \mathrm{S}^{++}(\mathbb{E}))$ is denoted by

$$\lambda^*(\mathcal{M}) := \max_{\mathbf{p}\in\overline{\Omega},\, \|\dot{\mathbf{p}}\|=1} \|\dot{\mathbf{p}}\|_{\mathcal{M}(\mathbf{p})}. \tag{27}$$

Proposition 2.4. *Let* $\mathcal{M} \in C^0(\overline{\Omega}, \mathrm{S}^{++}(\mathbb{E}))$ *be a Riemannian metric, and for all* $\mathbf{p} \in \overline{\Omega}$ *let* $\mathcal{D}(\mathbf{p}) := \mathcal{M}(\mathbf{p})^{-1}$ *and* $(\rho_i(\mathbf{p}), \dot{\mathbf{e}}_i(\mathbf{p}))_{i=1}^{d'}$ *be as in* (13). *Then the scheme* $\mathfrak{F}_h$ *defined by* (26) *is monotone and causal. In addition:*

(i) The null map $U = 0$ *satisfies* $\mathfrak{F}_h U \equiv 0$, *hence is a sub-solution to the scheme* $\mathfrak{F}_h - 1$.

(ii) Let $R > 0$ be such that Ω is contained in the ball of radius $R - hr_*$ and centered at the origin, and let $U(\mathbf{p}) := R - \|\mathbf{p}\|$, for all $\mathbf{p} \in \Omega_h$. Then for all $\lambda \geq 0$, and all $\mathbf{p} \in \Omega_h$

$$\mathfrak{F}_h U(\mathbf{p}) \geq \|\mathbf{p}/\|\mathbf{p}\|\|_{\mathcal{D}(\mathbf{p})},$$

where $\mathbf{p}/\|\mathbf{p}\|$ can be replaced with an arbitrary unit vector in the case $\mathbf{p} = 0$. As a result, λU is a super-solution to the scheme $\mathfrak{F}_h - 1$ for any $\lambda \geq \lambda^*(\mathcal{M})$.

(iii) If U is a super-solution to $\mathfrak{F}_h - 1$, then $(1+\varepsilon)U$ is a strict super-solution for any $\varepsilon > 0$.

Proof. The monotony and causality of the scheme $\mathfrak{F}_h$ immediatly follow from its expression (26). Point (i) is trivial, and point (iii) follows from the homogeneity property $\mathfrak{F}_h(\lambda U) = \lambda \mathfrak{F}_h U$. In the rest of this proof, the point $\mathbf{p} \in \Omega$ is regarded both as a vector in $\mathbb{E}$ and as a co-vector in $\mathbb{E}^*$, thanks to the euclidean structure of $\mathbb{E}$. For point (ii), we obtain by convexity of the euclidean norm, for any $\mathbf{p}, \dot{\mathbf{e}} \in \mathbb{E}$.

$$U(\mathbf{p}) - U(\mathbf{p} + \dot{\mathbf{e}}) = \|\mathbf{p} + \dot{\mathbf{e}}\| - \|\mathbf{p}\| \geq \langle \mathbf{p}/\|\mathbf{p}\|, \dot{\mathbf{e}} \rangle,$$

where $\mathbf{p}/\|\mathbf{p}\|$ can be replaced with any unit vector if $\mathbf{p} = 0$. Hence for all $\mathbf{p} \in \Omega_h$, as announced,

$$(\mathfrak{F}_h U(\mathbf{p}))^2 \geq \frac{1}{\|\mathbf{p}\|^2} \sum_{1 \leq i \leq d'} \rho_i(\mathbf{p}) \langle \mathbf{p}, \dot{\mathbf{e}}_i \rangle^2 = \frac{\|\mathbf{p}\|^2_{\mathcal{D}(\mathbf{p})}}{\|\mathbf{p}\|^2}.$$

Finally $\mathfrak{F}_h(\lambda U)(\mathbf{p}) \geq 1$ if $\lambda \geq \lambda^*(\mathcal{M})$ by the 1-homogeneity of $\mathfrak{F}$, and the observation that the least eigenvalue of $\mathcal{D}(\mathbf{p})$ is inverse of the largest eigenvalue of $\mathcal{M}(\mathbf{p})$. □

In the rest of this section, we establish the properties required to apply the doubling of variables argument, Theorem 2.3, to prove the second part of Theorem 1.3. The following proposition immediately implies that the exit time value function, denoted hereafter by u, is C^u_{Lip}-Lipschitz, with $C^u_{\mathrm{Lip}} := \lambda^*(\mathcal{M})$.

Proposition 2.5. *Let $\Omega \subseteq \mathbb{E}$ be an arbitrary bounded domain, equipped with a metric $\mathcal{F} : \overline{\Omega} \times \mathbb{E} \to \mathbb{R}$ such that $\mathcal{F}_{\mathbf{p}}(\dot{\mathbf{p}}) \leq C_0 \|\dot{\mathbf{p}}\|$ for any $\mathbf{p} \in \overline{\Omega}$, $\dot{\mathbf{p}} \in \mathbb{E}$. Then the distance u from $\partial\Omega$ is C_0-Lipschitz.*

Proof. Let $\mathbf{p}, \mathbf{q} \in \overline{\Omega}$, and let us prove that $u(\mathbf{q}) \leq u(\mathbf{p}) + C_0\|\mathbf{p} - \mathbf{q}\|$. Let $\gamma : [0,1] \to \mathbb{E}$ be the parametrization of the line segment $[\mathbf{p}, \mathbf{q}]$ at constant speed. If this segment intersects $\partial\Omega$, then denoting $T \in [0,1]$ the largest time such that $\gamma(T) \in \partial\Omega$ one has $u(\mathbf{q}) \leq \mathrm{Length}_{\mathcal{F}}(\gamma_{|[T,1]}) \leq C_0\|\mathbf{p} - \mathbf{q}\|$ as announced. Otherwise, denoting by $\tilde{\gamma}$ a minimal path from $\partial\Omega$ to $\mathbf{p}$ one has by path concatenation $u(\mathbf{q}) \leq \mathrm{length}_{\mathcal{F}}(\tilde{\gamma}) + \mathrm{length}_{\mathcal{F}}(\gamma) \leq u(\mathbf{p}) + C_0\|\mathbf{p} - \mathbf{q}\|$ as announced. □

In the rest of this section, we use the notations and assumptions of Theorems 1.3 and 2.3, except of course assumptions (i) and (ii) of the latter which we intend to prove, and denote by U_h is the solution to $\mathfrak{F}_h - 1$. In particular $\lambda \in [1/2, 1[$ and $\delta > 0$ are parameters from Theorem 2.3, and $(\overline{\mathbf{p}}, \overline{\mathbf{q}}), (\tilde{\mathbf{p}}, \tilde{\mathbf{q}}) \in \mathbb{E} \times h\mathbb{L}$ are points pairs where the maxima $\overline{M}_{\lambda,\delta}, \widetilde{M}_{\lambda,\delta}$ are attained.

Establishing assumption (i) of Theorem 2.3. Our first lemma is a direct application of the definition of sub- and super-solutions of HJB PDEs and monotone discretization schemes.

Lemma 2.6. *Let* $\overline{\mathbf{w}} := (\overline{\mathbf{p}} - \overline{\mathbf{q}})/\delta$, *and let* $\overline{U}(\mathbf{p}) := \langle \overline{\mathbf{w}}, \mathbf{p} \rangle + \frac{1}{2\delta}\|\mathbf{p} - \overline{\mathbf{p}}\|^2$ *for all* $\mathbf{p} \in h\mathbb{L}$. *Then*

$$\mathfrak{F}_h \overline{U}(\overline{\mathbf{p}}) \leq \lambda, \qquad\qquad \|\overline{\mathbf{w}}\|_{\mathcal{D}(\overline{\mathbf{q}})} \geq 1. \tag{28}$$

Let $\tilde{\mathbf{w}} := (\tilde{\mathbf{p}} - \tilde{\mathbf{q}})/\delta$, *and let* $\tilde{U}(\mathbf{p}) := \langle \tilde{\mathbf{w}}, \mathbf{p} \rangle - \frac{1}{2\delta}\|\mathbf{p} - \tilde{\mathbf{p}}\|^2$ *for all* $\mathbf{p} \in h\mathbb{L}$. *Then*

$$\mathfrak{F}_h \tilde{U}(\tilde{\mathbf{p}}) \geq 1, \qquad\qquad \|\tilde{\mathbf{w}}\|_{\mathcal{D}(\tilde{\mathbf{q}})} \leq \lambda. \tag{29}$$

Here and below we regard $\overline{\mathbf{w}}$ *and* $\tilde{\mathbf{w}}$ *as co-vectors, using the euclidean structure of* $\mathbb{E}$.

Proof. Note that the scheme $\mathfrak{F}_h$ is here (slightly abusively) applied to the functions $\overline{U}$, $\tilde{U}$, which are non-zero over $h\mathbb{L} \setminus \Omega_h$. We focus on the proof of (28), the case of (29) being similar. By definition of $\overline{M}_{\lambda,\delta}$, the function

$$\mathbf{p} \in h\mathbb{L} \mapsto \lambda U_h(\mathbf{p}) - u(\overline{\mathbf{q}}) - \frac{1}{2\delta}\|\mathbf{p} - \overline{\mathbf{q}}\|^2 = \lambda U_h(\mathbf{p}) - \overline{U}(\mathbf{p}) - K$$

attains its maximum at $\overline{\mathbf{p}}$, where $K = \overline{u}(\overline{\mathbf{q}}) - \frac{1}{2}\langle \overline{\mathbf{w}}, \overline{\mathbf{p}} + \overline{\mathbf{q}} \rangle$ is independent of the variable $\mathbf{p}$. Hence for all $\mathbf{p} \in h\mathbb{L}$

$$\lambda U_h(\overline{\mathbf{p}}) - \overline{U}(\overline{\mathbf{p}}) - K \geq \lambda U_h(\mathbf{p}) - \overline{U}(\mathbf{p}) - K, \quad \text{equivalently } U_h(\overline{\mathbf{p}}) - U_h(\mathbf{p}) \geq U(\overline{\mathbf{p}})/\lambda - \overline{U}(\mathbf{p})/\lambda.$$

By monotony of the scheme $\mathfrak{F}_h$, see Definition 2.1, we obtain $\mathfrak{F}_h(\overline{U}/\lambda)(\overline{\mathbf{p}}) \leq \mathfrak{F}_h U_h(\overline{\mathbf{q}}) = 1$, hence (28, left) by the homogeneity of $\mathfrak{F}_h$. Likewise, defining $\overline{u}(\mathbf{q}) := \langle \overline{\mathbf{w}}, \mathbf{q} \rangle - \frac{1}{2\delta}\|\mathbf{q} - \overline{\mathbf{q}}\|^2$ for all $\mathbf{q} \in \mathbb{E}$, the function

$$\mathbf{q} \in \mathbb{E} \mapsto \lambda U_h(\overline{\mathbf{p}}) - u(\mathbf{q}) - \frac{1}{2\delta}\|\mathbf{p} - \overline{\mathbf{q}}\|^2 = \overline{u}(\mathbf{q}) - u(\mathbf{q}) - K'$$

attains its minimum at $\overline{\mathbf{q}}$, where K' is the adequate constant. Since u is a (super-)solution to the PDE (12), this implies $1 \leq \|\mathrm{d}\overline{u}(\overline{\mathbf{q}})\|_{\mathcal{D}(\overline{\mathbf{q}})} = \|\overline{\mathbf{w}}\|_{\mathcal{D}(\overline{\mathbf{q}})}$, which concludes the proof. □

The following lemma assumes *for contradiction* that $(\overline{\mathbf{p}}, \overline{\mathbf{q}}) \in \Omega_h \times \Omega$ and obtains estimates *contradicting* Lemma 2.6, provided λ is above a certain bound, which is assumed in the following. Therefore $(\overline{\mathbf{p}}, \overline{\mathbf{q}}) \notin \Omega_h \times \Omega$, by contradiction, and likewise $(\tilde{\mathbf{p}}, \tilde{\mathbf{q}}) \notin \Omega_h \times \Omega$, by a similar argument, which establishes assumption (ii) of Theorem 2.3.

Let $C^{\mathcal{D}}_{\mathrm{Lip}}$ be a constant such that for all $\mathbf{p}, \mathbf{q} \in \overline{\Omega}$ and all $\hat{\mathbf{p}} \in \mathbb{E}^*$

$$|\|\hat{\mathbf{p}}\|_{\mathcal{D}(\mathbf{p})} - \|\hat{\mathbf{p}}\|_{\mathcal{D}(\mathbf{q})}| \leq C^{\mathcal{D}}_{\mathrm{Lip}} \|\mathbf{p} - \mathbf{q}\| \|\hat{\mathbf{p}}\|. \tag{30}$$

Such a constant exists by the Lipschitz regularity of the metric $\mathcal{M}$, assumed in Theorem 1.3.

Lemma 2.7. *Assume that* $(\overline{\mathbf{p}}, \overline{\mathbf{q}}) \in \Omega_h \times \Omega$ *and define* $\overline{\mathbf{w}}$ *and* $\overline{U}$ *as in Lemma 2.6. Then*

$$\left|\mathfrak{F}_h \overline{U}(\overline{\mathbf{p}}) - \|\overline{\mathbf{w}}\|_{\mathcal{D}(\overline{\mathbf{p}})}\right| \leq C_1 r_* \frac{h}{\delta}, \qquad\qquad \left|\|\overline{\mathbf{w}}\|_{\mathcal{D}(\overline{\mathbf{q}})} - \|\overline{\mathbf{w}}\|_{\mathcal{D}(\overline{\mathbf{p}})}\right| \leq C_2 \delta, \tag{31}$$

with $C_1 := \lambda^*(\mathcal{D})\sqrt{d}$ *and* $C_2 := (4C^u_{\mathrm{Lip}})^2 C^{\mathcal{D}}_{\mathrm{Lip}}$. *This contradicts* (28) *unless* $\lambda \geq 1 - C_1 r_* h/\delta - C_2\delta$. *The same estimates and conclusion hold for* $\tilde{\mathbf{w}}$ *and* $\tilde{U}$ *if* $(\tilde{\mathbf{p}}, \tilde{\mathbf{q}}) \in \Omega_h \times \Omega$.

Proof. We focus on the case of $(\overline{\mathbf{p}}, \overline{\mathbf{q}})$, the second case of $(\tilde{\mathbf{p}}, \tilde{\mathbf{q}})$ being similar, and begin with the proof of (31, left) which contains the key technical points. By definition of the quadratic function $\overline{U}$, one has

$$\max\{0, \overline{U}(\overline{\mathbf{p}}) - \overline{U}(\overline{\mathbf{p}} + h\dot{\mathbf{e}}_i), \overline{U}(\overline{\mathbf{p}}) - \overline{U}(\overline{\mathbf{p}} - h\dot{\mathbf{e}}_i)\} = h|\langle \overline{\mathbf{w}}, \dot{\mathbf{e}}_i \rangle| + \frac{h^2}{\delta}\|\dot{\mathbf{e}}_i\|^2, \tag{32}$$

for any $1 \leq i \leq d'$, where $(\rho_i(\overline{\mathbf{p}}), \dot{\mathbf{e}}_i)_{i=1}^{d'}$ are the weights and offsets of the discretization scheme at $\overline{\mathbf{p}}$, see (13). Denote by $m, w, e \in \mathbb{R}^{d'}$ the vectors of components respectively: m_i the LHS of (32), $w_i := |\langle \overline{\mathbf{w}}, \dot{\mathbf{e}}_i \rangle|$, and $e_i := \|\dot{\mathbf{e}}_i\|^2$, for all $1 \leq i \leq d'$. Introduce also the semi-norm $\|z\|_{\overline{\mathbf{p}}} := \sqrt{\sum_{i=1}^{d'} \rho_i(\overline{\mathbf{p}}) z_i^2}$ on $\mathbb{R}^{d'}$. Then one has

$$m = hw + \frac{h^2}{\delta} e, \qquad \mathfrak{F}_h \overline{U}(\overline{\mathbf{p}}) = h^{-1} \|m\|_{\overline{\mathbf{p}}} \qquad \|\overline{\mathbf{w}}\|_{\mathcal{D}(\overline{\mathbf{p}})} = \|w\|_{\overline{\mathbf{p}}},$$

and therefore $\left| \mathfrak{F}_h \overline{U}(\overline{\mathbf{p}}) - \|\overline{\mathbf{w}}\|_{\mathcal{D}(\overline{\mathbf{p}})} \right| = \left| \|w + \frac{h}{\delta} e\|_{\overline{\mathbf{p}}} - \|w\|_{\overline{\mathbf{p}}} \right| \leq \frac{h}{\delta} \|e\|_{\overline{\mathbf{p}}}$ by the triangular inequality. Finally observe that

$$\|e\|_{\overline{\mathbf{p}}}^2 = \sum_{1 \leq i \leq d'} \rho_i(\overline{\mathbf{p}}) \left(\|\dot{\mathbf{e}}_i\|^2 \right)^2 \leq \sum_{1 \leq i \leq d'} \rho_i(\overline{\mathbf{p}}) \|\dot{\mathbf{e}}_i\|^2 \max_{1 \leq i \leq d'} \|\dot{\mathbf{e}}_i\|^2 = \mathrm{Tr}(\mathcal{D}(\overline{\mathbf{p}})) r_*^2,$$

where Tr denotes the trace of a matrix. The announced result (31, left) then follows from $\mathrm{Tr}(\mathcal{D}(\mathbf{p})) \leq d(\lambda^*(\mathbf{p}))^2$.

The second estimate (31, right) follows from the Lipschitz regularity of the metric (30), together with the upper bound $\|\overline{\mathbf{p}} - \overline{\mathbf{q}}\| \leq 4C^u_{\mathrm{Lip}} \delta$ established in Theorem 2.3, which implies $\|\overline{\mathbf{w}}\| \leq 4C^u_{\mathrm{Lip}}$. Combining these estimates with Lemma 2.6 yields

$$\lambda + C_1 r_* h/\delta \geq \|\overline{\mathbf{w}}\|_{\mathcal{D}(\overline{\mathbf{p}})} \geq 1 - C_2 \delta,$$

which implies the announced lower bound for λ. The same estimates can be derived in the second case, and with Lemma 2.6 they imply $1 - C_1 r_* h/\delta \leq \|\tilde{\mathbf{w}}\|_{\mathcal{D}(\tilde{\mathbf{p}})} \leq \lambda + C_2 \delta$ which yields the same lower bound for λ. □

Establishing assumption (ii) of Theorem 2.3. The controlled growth of the discrete solution U_h close to $\partial\Omega$, assumption (ii) of Theorem 2.3, is established in the Proposition 2.10. Note that the assumptions of Theorem 1.3 are too weak to prove a global Lipschitz type estimate for U_h, as in e.g. [5, 18], and actually cannot exclude a staggered grid effect (never observed in practice) far from $\partial\Omega$. The idea underlying this proof is to construct from any point in $\mathbf{p}_0 \in \Omega_h$ sufficiently close to $\partial\Omega$, a short chain of neighbors $\mathbf{p}_1, \cdots, \mathbf{p}_n$ ending in $\partial\Omega_h$ and connected by offsets of the numerical scheme $\mathbf{p}_{i+1} = \mathbf{p}_i + h\dot{\mathbf{e}}_i(\mathbf{p}_i)$ which associated weights $\rho_i(\mathbf{p}_i)$ are positively bounded below; this is the discrete counterpart of a short time local control to the to boundary [2].

Our first step is to provide a precise definition to the *exterior cone condition* assumed in the statement of Theorem 1.3.

Definition 2.8 (Exterior cone condition)**.** *The domain $\Omega \subseteq \mathbb{E}$ obeys an exterior cone condition iff there exists constants C_Ω and $c_\Omega > 0$ such that for all $h \leq c_\Omega$,*

$$\forall \mathbf{p} \in \partial\Omega, \ \exists \mathbf{q} \in B(\mathbf{p}, C_\Omega h), \ \textit{such that } B(\mathbf{q}, h) \subseteq \mathbb{E} \setminus \Omega,$$

where $B(\mathbf{q}, h)$ denotes the open ball of center $\mathbf{q}$ and radius h.

The next technical compares the euclidean norm to its first order Taylor expansion.

Lemma 2.9. *For any $\mathbf{p}, \dot{\mathbf{e}} \in \mathbb{E}$ with $\mathbf{p} \neq 0$, one has $\|\mathbf{p} + \dot{\mathbf{e}}\| \leq \|\mathbf{p}\| + (\mathbf{p} \cdot \dot{\mathbf{e}})/\|\mathbf{p}\| + \|\dot{\mathbf{e}}\|^2/(2\|\mathbf{p}\|)$.*

Proof. Multiplying both sides by $\|\mathbf{p}\|$ and rearranging terms the statement is found equivalent to $\|\mathbf{p}\|\|\mathbf{p} + \dot{\mathbf{e}}\| \leq \frac{1}{2}(\|\mathbf{p}\|^2 + \|\mathbf{p} + \dot{\mathbf{e}}\|^2)$, equivalently to $0 \leq (\|\mathbf{p}\| - \|\mathbf{p} + \dot{\mathbf{e}}\|)^2$ which holds true. □

In the following proposition, we let $\mathrm{Cond}(\mathcal{D}) := \max\{\mathrm{Cond}(\mathcal{D}(\mathbf{p});\, \mathbf{p} \in \overline{\Omega}\}$, where the condition number of a symmetric matrix is defined in (4).

Proposition 2.10. *Let $\mathbf{p} \in \Omega_h$, and let $\mathbf{q} \in \mathbb{E}$ be such that $\|\mathbf{p}-\mathbf{q}\| \geq C_0 r_* h$, with $C_0 := \mathrm{Cond}(\mathcal{D})\sqrt{d'}$. Then there exists $1 \leq i \leq d'$ and a sign $s \in \{-1,1\}$ such that*

$$U_h(\mathbf{p}) \leq U_h(\mathbf{p} + hs\dot{\mathbf{e}}_i) + hC_1\|\dot{\mathbf{e}}_i\|, \qquad \text{and } \|\mathbf{p} + hs\dot{\mathbf{e}}_i - \mathbf{q}\| \leq \|\mathbf{p}-\mathbf{q}\| - hc_2\|\dot{\mathbf{e}}_i\|, \tag{33}$$

with $C_1 := \lambda^*(\mathcal{M})\sqrt{d'}$, $c_2 := 1/(2\,\mathrm{Cond}(\mathcal{D})\sqrt{d'})$. This implies assumption (ii) of Theorem 2.3, with the constants $C^U_{\mathrm{bd}} = C_1/c_2$, $C'^U_{\mathrm{bd}} := C^U_{\mathrm{bd}} C_\Omega C_0 r_*$, and $c_{\mathrm{bd}} = +\infty$.

Proof. Denote by $(\lambda_*)^2$ and $(\lambda^*)^2$ the smallest and largest eigenvalue of $\mathcal{D}(\mathbf{p})$ respectively. Let $\mathbf{n} := (\mathbf{q}-\mathbf{p})/\|\mathbf{q}-\mathbf{p}\|$, regarded as a co-vector thanks to the euclidean structure of $\mathbb{E}$. Then

$$\lambda_*^2 \leq \|\mathbf{n}\|^2_{\mathcal{D}(\mathbf{p})} = \sum_{1\leq i\leq d'} \rho_i(\mathbf{p})\langle \mathbf{n}, \dot{\mathbf{e}}_i\rangle^2. \tag{34}$$

Fix $1 \leq i \leq d'$ such that $\rho_i(\mathbf{p})\langle \mathbf{n}, \dot{\mathbf{e}}_i\rangle^2 \geq \lambda_*^2/d'$. Denote $\rho^2 := \rho_i(\mathbf{p})$, and $\dot{\mathbf{e}} := s\dot{\mathbf{e}}_i$ where s is the sign of $\langle \mathbf{n}, \dot{\mathbf{e}}_i\rangle$. One has, using that $\rho^2 \dot{\mathbf{e}} \otimes \dot{\mathbf{e}} \preceq \mathcal{D}(\mathbf{p}) \preceq (\lambda^*)^2\,\mathrm{Id}$ for the second inquality

$$\rho\langle \mathbf{n}, \dot{\mathbf{e}}\rangle \geq \lambda_*/\sqrt{d'} \qquad\qquad \rho\|\dot{\mathbf{e}}\| \leq \lambda^* \tag{35}$$

By definition of the discretization scheme (26) one has $h^{-2}\rho^2 \max\{0, U_h(\mathbf{p}) - U_h(\mathbf{p}+\dot{\mathbf{e}})\}^2 \leq (\mathfrak{F}_h U_h(\mathbf{p}))^2 = 1$, hence using (35, left) we obtain (33, left):

$$U(\mathbf{p}) - U(\mathbf{p}+\dot{\mathbf{e}}) \leq \frac{h}{\rho} \leq h\frac{\|\dot{\mathbf{e}}\|\sqrt{d'}}{\lambda_*}. \tag{36}$$

By (35) and $\mathrm{Cond}(\mathcal{D}) \geq \lambda^*/\lambda_*$ one has $\langle \mathbf{n}, \dot{\mathbf{e}}\rangle \geq \|\dot{\mathbf{e}}\|/(\mathrm{Cond}(\mathcal{D})\sqrt{d'})$. Denote $\mathbf{r} := (\mathbf{p}-\mathbf{q})/h$ and observe that by assumption $\|\mathbf{r}\| \geq C_0 r_* \geq \mathrm{Cond}(\mathcal{D})\sqrt{d'}\|\dot{\mathbf{e}}\|$ and definition of the max stencil radius r_*, see (14). Using Lemma 2.9 we obtain (33, right):

$$\|\mathbf{r}+\dot{\mathbf{e}}\| \leq \|\mathbf{r}\| - \langle \mathbf{n}, \dot{\mathbf{e}}\rangle + \frac{\|\dot{\mathbf{e}}\|^2}{2\|\mathbf{r}\|} \leq \|\mathbf{r}\| - \frac{\|\dot{\mathbf{e}}\|}{\mathrm{Cond}(\mathcal{D})\sqrt{d'}} + \frac{\|\dot{\mathbf{e}}\|}{2C_0}\frac{\|\dot{\mathbf{e}}\|}{r_*} \leq \|\mathbf{r}\| - \frac{\|\dot{\mathbf{e}}\|}{2\,\mathrm{Cond}(\mathcal{D})\sqrt{d'}}.$$

Finally, we conclude the proof of assumption (ii). Let $\mathbf{p}_0 \in \Omega_h$. Let $\mathbf{q}_* \in \partial\Omega$ be the closest point to $\mathbf{p}_0$, and let $\mathbf{q} \in B(\mathbf{q}_*, C_\Omega C_0 r_* h)$ be such that $B(\mathbf{q}, C_0 r_* h) \subseteq \mathbb{E} \setminus \Omega$. By the above argument, there exists a finite sequence of points $\mathbf{p}_1, \cdots, \mathbf{p}_{k-1} \in \Omega_h$, $\mathbf{p}_k \in \partial\Omega_h$, such that $U(\mathbf{p}_i) \leq U(\mathbf{p}_{i+1}) + C_1\delta_i$ and $\|\mathbf{p}_{i+1}-\mathbf{q}\| \leq \|\mathbf{p}_i - \mathbf{q}\| - c_2\delta_i$, denoting $\delta_i := \|\mathbf{p}_{i+1}-\mathbf{p}_i\|$, for all $0 \leq i < k$. Since $U(\mathbf{p}_k) = 0$ we obtain $U(\mathbf{p}_0) \leq C_1(\delta_0 + \cdots + \delta_{k-1})$, and since $\|\mathbf{p}_k - \mathbf{q}\| \geq 0$ we obtain $c_2(\delta_0 + \cdots + \delta_{k-1}) \leq \|\mathbf{p}_0 - \mathbf{q}\| \leq \|\mathbf{p}_0 - \mathbf{q}_*\| + C_\Omega C_0 r_* h$. Hence finally, as announced

$$U(\mathbf{p}_0) \leq (C_1/c_2)(d_{\partial\Omega}(\mathbf{p}_0) + C_\Omega C_0 r_* h). \qquad \square$$

3 Convergence in the sub-Riemannian case

This section is devoted to the proof of Theorem 1.9, the numerical analysis of the proposed scheme in the sub-Riemannian (or pre-Riemannian) setting. The estimates of $u - u_\varepsilon$ and $u_\varepsilon - U_{h,\varepsilon}$, respectively related to the model relaxation and to its discretization, are presented separately in §3.1 and §3.2. The arguments used to prove the Lipschitz regularity of u and to control the growth of $U_{h,\varepsilon}$ close to $\partial\Omega$ substantially differ from those used in the Riemannian case.

Before turning to these proofs, we recall two basic results on the regularity of the orthogonal projection onto a set, assumed respectively to be convex or to have a smooth boundary. Let $d_B(\mathbf{p}) := \min_{\mathbf{q}\in B} \|\mathbf{p}-\mathbf{q}\|$ the distance to a non-empty closed set $B \subseteq \mathbb{E}$, and let $\mathrm{P}_B(\mathbf{p})$ denote the minimizer $\mathbf{q} \in B$ for $d_B(\mathbf{p})$, when it is unique. The Haussdorff distance between two closed subsets of $\mathbb{E}$ is denoted $\mathcal{H}(\cdot,\cdot)$.

Proposition 3.1. *Let $\mathbf{p}, \mathbf{p}' \in \mathbb{E}$, and let $B, B' \subseteq \mathbb{E}$ be non-empty closed and convex. Then*

$$\|\mathrm{P}_B(\mathbf{p}) - \mathrm{P}_B(\mathbf{p}')\| \le \|\mathbf{p}-\mathbf{p}'\|, \quad \|\mathrm{P}_B(\mathbf{p}) - \mathrm{P}_{B'}(\mathbf{p})\| \le \sqrt{\mathcal{H}(B,B')}\sqrt{d_B(\mathbf{p}) + d_{B'}(\mathbf{p})}. \quad (37)$$

Proof. The uniqueness and Lipschitz regularity of the projection onto a convex set (37, left), are extremely classical hence their proof is omitted. *Proof of (37, right).* Let $\mathbf{q} := \mathrm{P}_B(\mathbf{p})$ and $\mathbf{q}' := \mathrm{P}_{B'}(\mathbf{p})$. We first assume that $\mathbf{p} \neq \mathbf{q}$, and regard $\mathbf{q}-\mathbf{p}$ as a co-vector by Riez duality. Observe that B is contained in the half space $H := \{\mathbf{r} \in \mathbb{E};\ \langle \mathbf{q}-\mathbf{p}, \mathbf{r}-\mathbf{q}\rangle \ge 0\}$, hence

$$\mathcal{H}(B,B') \ge d_B(\mathbf{q}') \ge d_H(\mathbf{q}') = \max\left\{0, \left\langle \frac{\mathbf{q}-\mathbf{p}}{\|\mathbf{q}-\mathbf{p}\|}, \mathbf{q}-\mathbf{q}' \right\rangle\right\} \ge \langle \mathbf{q}-\mathbf{p}, \mathbf{q}-\mathbf{q}'\rangle / d_B(\mathbf{p}).$$

Thus $d_B(\mathbf{p})\mathcal{H}(B,B') \ge \langle \mathbf{q}-\mathbf{p}, \mathbf{q}-\mathbf{q}'\rangle$, and this inequality also holds without the assumption $\mathbf{q} \neq \mathbf{p}$. Summing this identity with the similar one obtained exchanging the roles of (B,B') and $(\mathbf{q},\mathbf{q}')$ we obtain $(d_B(\mathbf{p}) + d_{B'}(\mathbf{p}))\mathcal{H}(B,B') \ge \langle (\mathbf{q}-\mathbf{p}) + (\mathbf{p}-\mathbf{q}'), \mathbf{q}-\mathbf{q}'\rangle = \|\mathbf{q}-\mathbf{q}'\|^2$ which is the announced result. □

Here and below, slightly abusively, we regard normal vectors to $\partial\Omega$ as co-vectors.

Proposition 3.2. *Assume that the domain boundary $\partial\Omega$ admits outward normals $\mathbf{n}(\mathbf{q})$, $\mathbf{q} \in \partial\Omega$, which have $1/R_\Omega$-Lipschitz regularity w.r.t. $\mathbf{q}$. Then $P_{\partial\Omega}(\mathbf{p})$ is uniquely defined for all $\mathbf{p} \in \mathbb{E}$ such that $d_{\partial\Omega}(\mathbf{p}) < R_\Omega$. Furthermore $d_{\partial\Omega}(\mathbf{p}+\dot{\mathbf{e}})$, for $\mathbf{p}, \dot{\mathbf{e}} \in \mathbb{E}$, is either zero or obeys*

$$d_{\partial\Omega}(\mathbf{p}+\dot{\mathbf{e}}) \le d_{\partial\Omega}(\mathbf{p}) + \langle \mathbf{n}(\mathbf{p}), \dot{\mathbf{e}}\rangle + \frac{\|\dot{\mathbf{e}}\|^2}{2R_\Omega}, \qquad \textit{where } \mathbf{n}(\mathbf{p}) := \mathbf{n}(\mathrm{P}_B(\mathbf{p})).$$

Proof. The Lipschitz assumption on the normals implies, for any $\mathbf{q} \in \partial\Omega$, the inclusions $B(\mathbf{q} - R_\Omega\mathbf{n}(\mathbf{q}), R_\Omega) \subseteq \overline{\Omega}$ and $B(\mathbf{q} + R_\Omega\mathbf{n}(\mathbf{q}), R_\Omega) \subseteq \mathbb{E} \setminus \Omega$. Fix $\mathbf{p} \in \mathbb{E}$, and let $\mathbf{q} \in \partial\Omega$ be an arbitrary closest point to $\mathbf{p}$. The first inclusion implies the announced uniqueness when $d_{\partial\Omega}(\mathbf{p}) < R_\Omega$, and the second inclusion, together with Lemma 2.9 applied to $\|(\mathbf{q} + R_\Omega\mathbf{n}(\mathbf{q}) - \mathbf{p}) - \dot{\mathbf{e}}\|$, implies the distance estimate. □

3.1 Estimating $u_\varepsilon - u$

In this subsection we bound, in the uniform norm, the difference between the value function u of the pre-Riemannian problem, and the one u_ε associated to the Riemannian approximation (18), for any $0 < \varepsilon \le 1$. Assumption 1.7, on global controllability and short time local controllability at the boundary, is central in the proof. Related arguments can be found in [2], but the proof is provided for completeness and because in the process we establish estimates used in §3.2. We use the notations and assumptions of Theorem 1.9. Let us introduce the control sets of the Riemannian relaxation

$$\mathcal{B}_\varepsilon(\mathbf{p}) := \{\dot{\mathbf{p}} \in \mathbb{E};\ \|\dot{\mathbf{p}}\|_{\mathcal{M}_\varepsilon(\mathbf{p})} \le 1\}$$

for each $0 < \varepsilon \le 1$, $\mathbf{p} \in \overline{\Omega}$, with the convention that $\mathcal{B}_0$ denotes the pre-Riemannian control sets of Definition 1.6. Note the inclusion $\mathcal{B}_\varepsilon(\mathbf{p}) \subseteq \mathcal{B}_{\varepsilon'}(\mathbf{p})$ for any $0 \le \varepsilon \le \varepsilon' \le 1$, which implies the

pointwise inequalities $T_{\mathcal{B}_\varepsilon}(\mathbf{p},\mathbf{q}) \geq T_{\mathcal{B}_{\varepsilon'}}(\mathbf{p},\mathbf{q})$ for the control times, and $u_\varepsilon(\mathbf{p}) \geq u_{\varepsilon'}(\mathbf{p})$ for the exit times, for any $\mathbf{p},\mathbf{q} \in \overline{\Omega}$.

Our first lemma establishes the Lipschitz regularity of the control sets $\mathcal{B}_\varepsilon(\mathbf{p})$ and of the tensors $\mathcal{D}_\varepsilon(\mathbf{p})$ with respect to the position $\mathbf{p} \in \overline{\Omega}$ and the relaxation parameter $\varepsilon \in [0,1]$. The control sets regularity allows to apply Gronwall's Lemma in the proof of Proposition 3.4, whereas the tensors regularity is used in §3.2 for establishing Assumption (i) of the doubling of variables argument Theorem 2.3. Denote by $A_\varepsilon(\mathbf{p})$ the matrix of columns $\dot{\omega}_1, \cdots, \dot{\omega}_n, \varepsilon\dot{\omega}_1^*, \cdots, \varepsilon\dot{\omega}_{n^*}^*$, for all $0 \leq \varepsilon \leq 1$, $\mathbf{p} \in \overline{\Omega}$. Since the these vector fields are Lipschitz and bounded, the matrix field A_ε obeys for some constant $C^{\mathcal{D}}_{\mathrm{Lip}}$ the following Lipschitz regularity property: for all $\mathbf{p},\mathbf{q} \in \overline{\Omega}$ and all $\varepsilon,\varepsilon' \in [0,1]$

$$\max\{\|A_\varepsilon(\mathbf{p}) - A_{\varepsilon'}(\mathbf{q})\|,\ \|A_\varepsilon^{\mathrm{T}}(\mathbf{p}) - A_{\varepsilon'}^{\mathrm{T}}(\mathbf{q})\|\} \leq C^{\mathcal{D}}_{\mathrm{Lip}}(\|\mathbf{p}-\mathbf{q}\| + |\varepsilon - \varepsilon'|). \tag{38}$$

Recall that the operator norm of an $m \times n$ matrix A is defined by $\|A\| := \sup\{\|A\dot{\mathbf{r}}\|;\ \dot{\mathbf{r}} \in \mathbb{R}^n,\ \|\dot{\mathbf{r}}\| \leq 1\}$. One easily checks that $\|A\| = \|A^{\mathrm{T}}\|$ for any matrix A, hence the l.h.s. of (38) could be slightly simplified, but we prefer to emphasize the fact that both the regularity of the matrix field A_ε and of its transpose are used.

Lemma 3.3. *One has the Lipschitz regularity: for all $\mathbf{p},\mathbf{q} \in \overline{\Omega}$, $\varepsilon,\varepsilon' \in [0,1]$, and all $\hat{\mathbf{r}} \in \mathbb{E}^*$*

$$\mathcal{H}(\mathcal{B}_\varepsilon(\mathbf{p}), \mathcal{B}_{\varepsilon'}(\mathbf{q})) \leq C^{\mathcal{D}}_{\mathrm{Lip}}(\|\mathbf{q}-\mathbf{p}\| + |\varepsilon - \varepsilon'|) \tag{39}$$

$$\big|\|\hat{\mathbf{r}}\|_{\mathcal{D}_\varepsilon(\mathbf{p})} - \|\hat{\mathbf{r}}\|_{\mathcal{D}_{\varepsilon'}(\mathbf{q})}\big| \leq C^{\mathcal{D}}_{\mathrm{Lip}}(\|\mathbf{q}-\mathbf{p}\| + |\varepsilon - \varepsilon'|)\|\hat{\mathbf{r}}\|. \tag{40}$$

Proof. For any maps φ,ψ from an arbitrary space X to $\mathbb{E}$, one has $\mathcal{H}(\varphi(X),\psi(X)) \leq \sup_{x\in X}\|\varphi(x) - \psi(x)\|$. Observing that $\mathcal{B}_\varepsilon(\mathbf{p}) = (A_\varepsilon(\mathbf{p}))(B)$, where B is the unit ball of $\mathbb{R}^{n+n^*}$, we obtain

$$\mathcal{H}(\mathcal{B}_\varepsilon(\mathbf{p}), \mathcal{B}_{\varepsilon'}(\mathbf{q})) \leq \sup_{x\in B}\|A_\varepsilon(\mathbf{p})x - A_{\varepsilon'}(\mathbf{q})x\| = \|A_\varepsilon(\mathbf{p}) - A_{\varepsilon'}(\mathbf{q})\| \leq C^{\mathcal{D}}_{\mathrm{Lip}}(\|\mathbf{q}-\mathbf{p}\| + |\varepsilon - \varepsilon'|).$$

which is (39). Observing that $\mathcal{D}_\varepsilon(\mathbf{p}) = A_\varepsilon(\mathbf{p})A_\varepsilon(\mathbf{p})^{\mathrm{T}}$, see Definition 1.6, we obtain (40), since

$$\big|\|\hat{\mathbf{r}}\|_{\mathcal{D}_\varepsilon(\mathbf{p})} - \|\hat{\mathbf{r}}\|_{\mathcal{D}_{\varepsilon'}(\mathbf{q})}\big| = \big|\|A_\varepsilon^{\mathrm{T}}(\mathbf{p})\hat{\mathbf{r}}\| - \|A_{\varepsilon'}^{\mathrm{T}}(\mathbf{q})\hat{\mathbf{r}}\|\big| \leq \|A_\varepsilon^{\mathrm{T}}(\mathbf{p}) - A_{\varepsilon'}^{\mathrm{T}}(\mathbf{q})\|\|\hat{\mathbf{r}}\|. \qquad \square$$

Proposition 3.4. *Let $0 \leq \varepsilon_0 \leq 1$, let $\gamma_0 : [0,T_0] \to \overline{\Omega}$ be a $\mathcal{B}_{\varepsilon_0}$-admissible path, and let $\mathbf{p}_0 := \gamma_0(0)$. Let $0 \leq \varepsilon_1 \leq 1$, and let $\gamma_1 : [0,T_1] \to \overline{\Omega}$ be a solution to the ODE*

$$\dot{\gamma}_1 := \mathrm{P}_{\mathcal{B}_{\varepsilon_1}(\gamma_1(t))}(\dot{\gamma}_0(t)),$$

with initial condition $\gamma_1(0) = \mathbf{p}_1 \in \Omega$, where the final time T_1 is either T_0 or the time where γ_1 reaches $\partial\Omega$. Then γ_1 is $\mathcal{B}_1$-admissible, and for any $0 \leq t \leq T_1$ one has

$$|\gamma_0(t) - \gamma_1(t)| \leq (|\mathbf{p}_0 - \mathbf{p}_1| + |\varepsilon_0 - \varepsilon_1|)\exp(C^{\mathcal{B}}_{\mathrm{Lip}}t) - |\varepsilon_0 - \varepsilon_1|.$$

Proof. The orthgonal projection $\mathrm{P}_B(\mathbf{p})$, of a given $\mathbf{p} \in \mathbb{E}$, depends continuously (in fact with (1/2)-Holder regularity) on the closed and convex set B, see Proposition 3.1. The right hand side of (3.4) therefore depends continuously on $\gamma_1(t)$, hence this ODE admits solutions by Peano's existence theorem. Note that the Picard-Lindelof/Cauchy-Lipschitz uniqueness theorem does *not* apply since it requires Lipschitz regularity of the r.h.s., but the lack of uniqueness is fortunately not an issue in this proof.

The $\mathcal{B}_{\varepsilon_1}$-admissibility of γ_1 holds by construction, and since $\dot{\gamma}_0(t) \in \mathcal{B}_{\varepsilon_0}(\gamma_0(t))$ one has

$$|\dot{\gamma}_0(t) - \dot{\gamma}_1(t)| \leq \mathcal{H}(\mathcal{B}_{\varepsilon_0}(\gamma_0(t)), \mathcal{B}_{\varepsilon_1}(\gamma_1(t))) \leq C^{\mathcal{B}}_{\mathrm{Lip}}(|\varepsilon_0 - \varepsilon_1| + |\gamma_0(t) - \gamma_1(t)|),$$

for any $0 \leq t \leq T_1$. The announced estimate then follows from Gronwall's lemma. $\square$

The following lemma makes use of transversality property in Assumption 1.7 to upper bound the exit time function u_ε close to the domain boundary $\partial\Omega$. This property is equivalent to: $\|\mathbf{n}(\mathbf{p})\|^2_{\mathcal{D}(\mathbf{p})} = \sum_{i=1}^n \langle \mathbf{n}(\mathbf{p}), \dot\omega_i(\mathbf{p})\rangle^2 \neq 0$ for all $\mathbf{p} \in \partial\Omega$, where $\mathbf{n}(\mathbf{p})$ denotes the outward normal to $\partial\Omega$. Hence denoting $\mathbf{n}(\mathbf{p}) := \mathbf{n}(\mathrm{P}_{\partial\Omega}(\mathbf{p}))$ for $\mathbf{p}$ close enough to $\partial\Omega$, as in Proposition 3.2, there exists by continuity positive constants $c_\mathcal{D}, c_\Omega$ such that

$$\|\mathbf{n}(\mathbf{p})\|_{\mathcal{D}(\mathbf{p})} \geq c_\mathcal{D}, \text{ for all } \mathbf{p} \in \overline{\Omega} \text{ such that } d_{\partial\Omega}(\mathbf{p}) \leq c_\Omega. \tag{41}$$

In the next lemma and proposition we construct paths from an arbitrary point $\mathbf{p} \in \overline{\Omega}$ to $\partial\Omega$, whereas the original problem (6) is to find a path from $\partial\Omega$ to $\mathbf{p}$. This change of orientation is only used for notational simplicity, and is valid since the paths can be reverse parametrized, and since the control sets are symmetric: $\mathcal{B}_\varepsilon(\mathbf{p}) = \{-\dot{\mathbf{p}};\ \dot{\mathbf{p}} \in \mathcal{B}_\varepsilon(\mathbf{p})\}$, for all $\mathbf{p} \in \overline{\Omega}$, $\varepsilon \in [0,1]$.

Lemma 3.5. *For all $\mathbf{p} \in \overline{\Omega}$ such that $d_{\partial\Omega}(\mathbf{p}) \leq c_\Omega$, one has $u(\mathbf{p}) \leq d_{\partial\Omega}(\mathbf{p})/c_\mathcal{D}$.*

Proof. Let $D\Omega := \{\mathbf{q} \in \overline{\Omega};\ d_{\partial\Omega}(\mathbf{q}) \leq c_\Omega\}$. Define a vector field $\dot{\mathbf{v}} : D\Omega \to \mathbb{E}$ by

$$\dot{\mathbf{v}}(\mathbf{q}) := \frac{\mathcal{D}(\mathbf{q})\mathbf{n}(\mathbf{q})}{\|\mathbf{n}(\mathbf{q})\|_{\mathcal{D}(\mathbf{q})}} = A_0(\mathbf{q})\frac{A_0^{\mathrm{T}}(\mathbf{q})\mathbf{n}(\mathbf{q})}{\|A_0^{\mathrm{T}}(\mathbf{q})\mathbf{n}(\mathbf{q})\|},$$

for all $\mathbf{q} \in D\Omega$, and note that $\dot{\mathbf{v}}(\mathbf{q}) \in \mathcal{B}(\mathbf{q})$. Consider the solution to the ODE $\dot\gamma(t) := \dot{\mathbf{v}}(\gamma(t))$, with initial condition $\gamma(0) = \mathbf{p} \in D\Omega$, stopping at the time $T \in [0,\infty]$ when γ leaves $D\Omega$. By construction, γ is a $\mathcal{B}_\varepsilon$-admissible path, and for all $0 \leq t \leq T$ one has by Proposition 3.2

$$\frac{d}{dt} d_{\partial\Omega}(\gamma(t)) = -\langle \mathbf{n}(\gamma(t)), \dot{\mathbf{v}}(\gamma(t))\rangle = -\|\mathbf{n}(\gamma(t))\|_{\mathcal{D}(\gamma(t))} \leq -c_\mathcal{D}.$$

Therefore $T \leq d_{\partial\Omega}/c_\mathcal{D}$ and $\gamma(T) \in \partial\Omega$, hence $u(\mathbf{p}) \leq T$ and the announced result follows. □

The following proposition establishes the Lipschitz regularity of $u_\varepsilon(\mathbf{p})$ with respect to both $\varepsilon \in [0,1]$ and $\mathbf{p} \in \overline{\Omega}$. Regularity w.r.t. ε proves (19, left) in Theorem 1.9, which was the aim of this section. Regularity w.r.t. $\mathbf{p}$ is used in the next subsection to apply the doubling of variables techniques.

Proposition 3.6. *One has the Lipschitz regularity property*

$$|u_{\varepsilon_0}(\mathbf{p}_0) - u_{\varepsilon_1}(\mathbf{p}_1)| \leq C^u_{\mathrm{Lip}}(\|\mathbf{p}_0 - \mathbf{p}_1\| + |\varepsilon_0 - \varepsilon_1|). \tag{42}$$

for all $\mathbf{p}_0, \mathbf{p}_1 \in \overline{\Omega}$ and all $\varepsilon_0, \varepsilon_1 \in [0,1]$, where $C^u_{\mathrm{Lip}} := \exp(C^\mathcal{B}_{\mathrm{Lip}}\|u\|_\infty)/c_\mathcal{D}$.

Proof. Assume w.l.o.g. that $u_{\varepsilon_0}(\mathbf{p}_0) \leq u_{\varepsilon_1}(\mathbf{p}_1)$. Let $\gamma_0 : [0, T_0] \to \overline{\Omega}$ be an optimal $\mathcal{B}_{\varepsilon_0}$-admissible path from $\mathbf{p}_0$ to $\partial\Omega$, where $T_0 := u_{\varepsilon_0}(\mathbf{p}_0)$. Let $\gamma_1 : [0, T_1] \to \overline{\Omega}$ be as in Proposition 3.4. If $\gamma_1(T_1) \in \partial\Omega$, then $u_1(\mathbf{p}_1) \leq T_1 \leq T_0$ and the result follows.

Otherwise by Proposition 3.4 we get $d_{\partial\Omega}(\gamma_1(T_0)) \leq \|\gamma_1(T_0) - \gamma_0(T_0)\| \leq C(|\varepsilon_0 - \varepsilon_1| + \|\mathbf{p}_0 - \mathbf{p}_1\|)$ with $C := \exp(C_{\mathrm{Lip}}T_0)$. Therefore

$$u_{\varepsilon_1}(\mathbf{p}_1) \leq T_0 + d_{\partial\Omega}(\gamma_1(T_0))/c_\mathcal{D} \leq u_{\varepsilon_0}(\mathbf{p}_0) + C^u_{\mathrm{Lip}}(\|\mathbf{p}_0 - \mathbf{p}_1\| + |\varepsilon_0 - \varepsilon_1|)$$

as announced, using Lemma 3.5 and recalling that $u_{\varepsilon_1} \leq u_0 = u$ on $\overline{\Omega}$, and assuming that $d_{\partial\Omega}(\gamma_1(T_0)) \leq c_\Omega$. Thus (42) holds for all $(\mathbf{p}_0, \varepsilon_0), (\mathbf{p}_1, \varepsilon_1) \in \overline{\Omega} \times [0,1]$ obeying $\|\mathbf{p}_0 - \mathbf{p}_1\| + |\varepsilon_0 - \varepsilon_1| \leq c_\Omega/C$. By defining $u_\varepsilon(\mathbf{p}) = 0$ for all $\mathbf{p} \in \mathbb{E} \setminus \Omega$, $\varepsilon \in [0,1]$, the result extends to all $(\mathbf{p}_0, \varepsilon_0), (\mathbf{p}_1, \varepsilon_1) \in \mathbb{E} \times [0,1]$ subject to the same closeness constraint, which finally can be removed since Lipschitz regularity on a convex set is a local property. □

3.2 Estimating $U_{h,\varepsilon} - u_\varepsilon$

In this subsection we complete the proof of Theorem 1.9 by estimating the difference $|U_{h,\varepsilon} - u_\varepsilon|$ on Ω_h, for any $h > 0$, $\varepsilon \in]0, 1]$, using the doubling of variables technique Theorem 2.3. We use the notations and assumptions of Theorems 1.9 and 2.3, except of course assumptions (i) and (ii) of the latter which we intend to prove.

The first assumption of Theorem 2.3 is the Lipschitz regularity of the value function u_ε, which is established in Proposition 3.6 above, with a constant C^u_{Lip} independent of ε. Note that, in contrast, naively adapting the Riemannian argument of Proposition 2.5 yields the Lipschitz constant $\lambda(\mathcal{M}_\varepsilon) \approx \varepsilon^{-1}$ exploding as $\varepsilon \to 0$, and thus unsuitable for proving Theorem 1.9.

The next step is to establish assumption (i) of Theorem 2.3. Lemma 2.6 from the Riemannian case applies without modification to u_ε and $U_{h,\varepsilon}$ since it does not involve quantitative properties of the Riemannian metric field $\mathcal{M}_\varepsilon$. Lemma 2.7 from the Riemannian case also applies, with constants independent of $\varepsilon \in]0, 1]$. Indeed the dual tensors have the expression $\mathcal{D}_\varepsilon = \mathcal{D} + \varepsilon^2 \mathcal{D}^*$, see (18), and therefore their max norm (27) is bounded $\lambda^*(\mathcal{D}_\varepsilon) \leq \lambda^*(\mathcal{D}_1)$ independently of $\varepsilon \in [0, 1]$. The last ingredient used to prove assumption (i) in the Riemannian case is the Lipschitz regularity of the dual norms (30), which is established in (40) for the pre-Riemannian model with a constant $C^{\mathcal{D}}_{\mathrm{Lip}}$ independent of $\varepsilon \in [0, 1]$.

The following proposition establishes assumption (ii) of Theorem 2.3, a discrete counterpart of short time local controllability at the boundary, by adapting the arguments developed in the Riemannian case, see Proposition 2.10. Note the use Assumption 1.7, which is required due to the lack of uniform definiteness of the the tensors $\mathcal{D}_\varepsilon$, $0 < \varepsilon \leq 1$. The weights and offsets used in the decomposition (13) of $\mathcal{D}_\varepsilon(\mathbf{p})$ are denoted $(\rho_{i,\varepsilon}(\mathbf{p}), \dot{\mathbf{e}}_{i,\varepsilon}(\mathbf{p}))_{i=1}^{d'}$, $\mathbf{p} \in \overline{\Omega}$, $0 < \varepsilon \leq 1$.

Proposition 3.7. *Let $\mathbf{p} \in \Omega_h$ be such that $d(\mathbf{p}, \partial\Omega) \leq c_\Omega$, and let $\varepsilon \in]0, 1]$. Then there exists $1 \leq i \leq d'$ and a sign $s \in \{-1, 1\}$ such that either $\mathbf{p} + hs\dot{\mathbf{e}}_{i,\varepsilon} \notin \Omega_h$ or*

$$U_{h,\varepsilon}(\mathbf{p}) \leq U_{h,\varepsilon}(\mathbf{p} + hs\dot{\mathbf{e}}_{i,\varepsilon}) + hC_1\|\dot{\mathbf{e}}_{i,\varepsilon}\|, \qquad d(\mathbf{p} + hs\dot{\mathbf{e}}_{i,\varepsilon}, \partial\Omega) \leq d(\mathbf{p}, \partial\Omega) - hc_2\|\dot{\mathbf{e}}_{i,\varepsilon}\|,$$

with $C_1 := \sqrt{d'}/c_{\mathcal{D}}$ and $c_2 := c_{\mathcal{D}}/(2\lambda^*(\mathcal{D}_1)\sqrt{d'})$. This implies assumption (ii) of Theorem 2.3, with the constants $C_{\mathrm{bd}} = C_1/c_2$, $C'_{\mathrm{bd}} := C_{\mathrm{bd}} r_\varepsilon$, and $c_{\mathrm{bd}} = c_{\mathcal{D}}$.

Proof. Using Assumption 1.7 and (41), one obtains a counterpart for (34)

$$c^2_{\mathcal{D}} \leq \|\mathbf{n}(\mathbf{p})\|^2_{\mathcal{D}_\varepsilon(\mathbf{p})} = \sum_{1 \leq i \leq d'} \rho_{i,\varepsilon}(\mathbf{p}) \langle \mathbf{n}(\mathbf{p}), \dot{\mathbf{e}}_{i,\varepsilon} \rangle^2,$$

where $\mathbf{n}(\mathbf{p}) := \mathbf{n}(\mathrm{P}_{\partial\Omega}(\mathbf{p}))$. The proof is then similar to the one of Proposition 2.10, up to the replacement of Lemma 2.9 with Proposition 3.2. □

4 Convergence in the Rander case

This section is devoted to proof of Theorem 1.11, namely the numerical analysis of the Rander metric variant of our PDE discretization scheme, using its notations and assumptions. Consider the scheme $\mathfrak{F}_h$ on the discrete domain Ω_h defined for any $U : \Omega_h \to \mathbb{R}$ and $\mathbf{p} \in \Omega_h$ by $(\mathfrak{F}_h U(\mathbf{p}))^2 :=$

$$h^{-2} \sum_{1 \leq i \leq d'} \rho_i(\mathbf{p}) \max\{0,\, U(\mathbf{p}) - U(\mathbf{p} + h\dot{\mathbf{e}}_i) + h\langle \hat{\eta}(\mathbf{p}), \dot{\mathbf{e}}_i \rangle,\, U(\mathbf{p}) - U(\mathbf{p} - h\dot{\mathbf{e}}_i) - h\langle \hat{\eta}(\mathbf{p}), \dot{\mathbf{e}}_i \rangle\}^2. \quad (43)$$

By convention, U is extended by 0 outside Ω_h. Note that this scheme is non-causal as soon as some of the terms $h\langle \hat{\eta}(\mathbf{p}), \dot{\mathbf{e}}_i \rangle$ are non-zero, see Definition 2.1, in contrast with (26).

Proposition 4.1. *The scheme* (43) *is monotone. In addition:*

(i) The null map $U = 0$ satisfies $\mathfrak{F}_h U(\mathbf{p}) = \|\hat{\eta}(\mathbf{p})\|^2_{\mathcal{D}(\mathbf{p})} < 1$ for all $\mathbf{p} \in \Omega_h$, hence it is a sub-solution for $\mathfrak{F}_h - 1$.

(ii) Let $R > 0$ be such that Ω is contained in the ball of radius $R - hr_*$, and let $U(\mathbf{p}) := R - \|\mathbf{p}\|$, for all $\mathbf{p} \in \Omega_h$. Then for all $\lambda \geq 0$, and all $\mathbf{p} \in \Omega_h$,

$$\mathfrak{F}_h(\lambda U)(\mathbf{p}) \geq \|\lambda \mathbf{p}/\|\mathbf{p}\| - \hat{\eta}(\mathbf{p})\|^2_{\mathcal{D}(\mathbf{p})},$$

where $\mathbf{p}/\|\mathbf{p}\|$ can be replaced with an arbitrary unit vector in the case $\mathbf{p} = 0$. Thus λU is a super-solution for all sufficiently large λ.

(iii) Let U is a super-solution for $\mathfrak{F}_h - 1$, and let $x_1, \cdots, x_N$ be the points of Ω_h ordered in such way that $U(\mathbf{x}_1) \leq \cdots \leq U(\mathbf{x}_N)$. For each $\varepsilon > 0$ let $V_\varepsilon : \Omega_h \to \mathbb{R}$ be defined by $V_\varepsilon(\mathbf{x}_i) = U(\mathbf{x}_i) + \varepsilon - \varepsilon^{1+i}$. Then V_ε is a strict super-solution to $\mathfrak{F}_h - 1$ for all sufficiently small ε.

Proof. Point (i) follows from the identity $\sum_{1 \leq i \leq d'} \rho_i(\mathbf{p}) \langle \hat{\eta}(\mathbf{p}), \dot{\mathbf{e}}_i \rangle^2 = \|\hat{\eta}(\mathbf{p})\|^2_{\mathcal{D}(\mathbf{p})}$, and the smallness assumption (20, right) on the co-vector field $\hat{\eta}$. Point (ii) is proved as in Proposition 2.4. Point (iii) is in contrast non-trivial. Let U be a super-solution for $\mathfrak{F}_h - 1$ and let $1 \leq k \leq N$. Denote by $m_i(\mathbf{p})$ the i-th maximum of three terms appearing in (43), so that $\mathfrak{F}_h U(\mathbf{p}) = \sum_{i=1}^{d'} \rho_i(\mathbf{p}) m_i(\mathbf{p})^2$ for each $\mathbf{p} \in \Omega_h$. Then one has the Taylor expansion

$$\mathfrak{F}_h V_\varepsilon(\mathbf{p}_k) - \mathfrak{F}_h U(\mathbf{p}_k) = 2 \sum_{1 \leq i \leq d'} \rho_i(\mathbf{p}_k) m_i(\mathbf{p}_k) (\varepsilon^{1+k_i} - \varepsilon^{1+k}) + \mathcal{O}(\varepsilon^{2+2k_*}), \tag{44}$$

where k_i is an integer depending on k and $i \in \{1, \cdots, d'\}$ and chosen so that $\mathbf{p}_{k_i} = \mathbf{p}_k$, (resp. $\mathbf{p}_{k_i} = \mathbf{p}_k + h\dot{\mathbf{e}}_i$, resp. $\mathbf{p}_{k_i} = \mathbf{p}_k - h\dot{\mathbf{e}}_i$) if the maximum defining $m_i(\mathbf{p}_k)$ is achieved for the first (resp. second, resp. third) term. (If this point is outside Ω_h, we let $k_i = 0$. In case of a tie, the point with smallest index is chosen.) Finally, $k_* := \min\{k_i;\, 1 \leq i \leq d'\}$.

We prove below that $k_i < k$ for some $1 \leq i \leq d'$, which by (44) implies that $\mathfrak{F}_h V_\varepsilon(\mathbf{p}_k) > \mathfrak{F}_h U(\mathbf{p}_k) \geq 1$ for all sufficiently small $\varepsilon > 0$ as announced. Assume for contradiction that $k_i \geq k$ for all $1 \leq i \leq d'$, hence that $U(\mathbf{p}_{k_i}) \geq U(\mathbf{p}_k)$ and therefore that $m_i(\mathbf{p}_k) \leq |\langle \hat{\eta}(\mathbf{p}_k), \dot{\mathbf{e}}_i \rangle|$ for all $1 \leq i \leq d'$. Then denoting $\mathbf{p} := \mathbf{p}_k$ one obtains

$$\mathfrak{F}_h U(\mathbf{p}) = \sum_{1 \leq i \leq d'} \rho_i(\mathbf{p}) m_i(\mathbf{p})^2 \leq \sum_{1 \leq i \leq d'} \rho_i(\mathbf{p}) \langle \hat{\eta}(\mathbf{p}), \dot{\mathbf{e}}_i \rangle^2 = \|\hat{\eta}(\mathbf{p})\|^2_{\mathcal{D}(\mathbf{p})} < 1,$$

in contradiction with our assumption that U is a super-solution for $\mathfrak{F}_h - 1$. The result follows. □

In the rest of this section, we establish the properties required to apply the doubling of variables argument Theorem 2.3, using its notations. The first ingredient is with the Lipschitz regularity of the exit time value function u. By construction the Rander metric (20) satisfies for all $\mathbf{p} \in \overline{\Omega}$ and all $\dot{\mathbf{p}} \in \mathbb{E}$.

$$\mathcal{F}_{\mathbf{p}}(\dot{\mathbf{p}}) = \|\dot{\mathbf{p}}\|_{\mathcal{M}(\mathbf{p})} + \langle \hat{\eta}(\mathbf{p}), \dot{\mathbf{p}} \rangle \leq (\lambda^*(\mathcal{M}) + \|\hat{\eta}\|_\infty) \|\dot{\mathbf{p}}\|.$$

Hence u is C^u_{Lip}-Lipschitz by Proposition 2.5, as desired, with constant $C^u_{\mathrm{Lip}} := \lambda^*(\mathcal{M}) + \|\hat{\eta}\|_\infty$ where the max-norm $\lambda^*(\mathcal{M})$ of a tensor field is defined in (27).

Establishing assumption (i) of Theorem 2.3. We proceed similarly to the Riemannian case §2.2, starting with an extension of Lemma 2.6 to Rander metrics. The proof, left to the reader, is similar up to fact that the scheme $\mathfrak{F}_h U$ and the PDE operator $\|\mathrm{d}u - \hat\eta\|_{\mathcal{D}}$ are not homogeneous w.r.t. their respective argument U and u. The variables $\lambda \in [1/2, 1[$, $\delta > 0$, $(\overline{\mathbf{p}}, \overline{\mathbf{q}}), (\tilde{\mathbf{p}}, \tilde{\mathbf{q}}) \in \Omega_h \times \Omega$ are from Theorem 2.3.

Lemma 4.2. *Let* $\overline{\mathbf{w}} := (\overline{\mathbf{p}} - \overline{\mathbf{q}})/\delta$ *and let* $\overline{U}(\mathbf{p}) := \langle \overline{\mathbf{w}}, \mathbf{p}\rangle + \frac{1}{2\delta}\|\mathbf{p} - \overline{\mathbf{p}}\|^2$, *for all* $\mathbf{p} \in \mathbb{L}_h$. *Then*

$$\mathfrak{F}_h(\overline{U}/\lambda)(\overline{\mathbf{p}}) \le 1 \qquad\qquad \|\overline{\mathbf{w}} - \hat\eta(\overline{\mathbf{q}})\|_{\mathcal{D}(\overline{\mathbf{q}})} \ge 1.$$

Let $\tilde{\mathbf{w}} := (\tilde{\mathbf{p}} - \tilde{\mathbf{q}})/\delta$ *and let* $\tilde{U}(\mathbf{p}) := \langle \tilde{\mathbf{w}}, \mathbf{p}\rangle - \frac{1}{2\delta}\|\mathbf{p} - \tilde{\mathbf{p}}\|^2$, *for all* $\mathbf{p} \in \mathbb{L}_h$. *Then*

$$\mathfrak{F}_h\tilde{U}(\tilde{\mathbf{p}}) \ge 1 \qquad\qquad \|\tilde{\mathbf{w}}/\lambda - \hat\eta(\tilde{\mathbf{q}})\|_{\mathcal{D}(\tilde{\mathbf{q}})} \le 1.$$

Let $C^{\mathcal{D}}_{\mathrm{Lip}}$ be a Lipschitz regularity constants for the tensors $\mathcal{D}$, in the sense of (30). Let also $C^{\hat\eta}_{\mathrm{Lip}}$ and $c_{\mathcal{D},\hat\eta} > 0$ be such that for all $\mathbf{p}, \mathbf{q} \in \overline{\Omega}$

$$\|\hat\eta(\mathbf{p}) - \hat\eta(\mathbf{q})\| \le C^{\hat\eta}_{\mathrm{Lip}}\|\mathbf{p} - \mathbf{q}\|, \qquad\qquad \|\hat\eta(\mathbf{p})\|_{\mathcal{D}(\mathbf{p})} \le 1 - c_{\mathcal{D},\hat\eta}.$$

Lemma 4.3. *Assume that* $(\overline{\mathbf{p}}, \overline{\mathbf{q}}) \in \Omega_h \times \Omega$ *and define* $\overline{\mathbf{w}}$ *and* $\overline{U}$ *as in Lemma 2.6. Then*

$$\Big|\mathfrak{F}_h\overline{(U/\lambda)}(\overline{\mathbf{p}}) - \|\overline{\mathbf{w}}/\lambda - \hat\eta(\overline{\mathbf{p}})\|_{\mathcal{D}(\overline{\mathbf{p}})}\Big| \le C_0 r_* \frac{h}{\delta}, \quad \big|\|\overline{\mathbf{w}} - \hat\eta(\overline{\mathbf{q}})\|_{\mathcal{D}(\overline{\mathbf{q}})} - \|\overline{\mathbf{w}} - \hat\eta(\overline{\mathbf{p}})\|_{\mathcal{D}(\overline{\mathbf{p}})}\big| \le C_1\delta, \tag{45}$$

with $C_0 := \lambda^*(\mathcal{D})\sqrt{d}$ *and* $C_1 := C^{\mathcal{D}}_{\mathrm{Lip}}(4C^u_{\mathrm{Lip}})(4C^u_{\mathrm{Lip}} + C^{\hat\eta}_{\mathrm{Lip}}) + \lambda^*(\mathcal{D})C^{\hat\eta}_{\mathrm{Lip}}$. *Assuming* $\delta \le c_{\mathcal{D},\hat\eta}/(2C_1)$ *this implies* $\lambda \ge 1 - \frac{2}{c_{\mathcal{D},\hat\eta}}(C_0 r_* \frac{h}{\delta} + C_1\delta)$. *The same estimates and conclusion hold for* $(\tilde{\mathbf{p}}, \tilde{\mathbf{q}})$.

Proof. We focus on the case of $(\overline{\mathbf{p}}, \overline{\mathbf{q}})$, the second case of $(\tilde{\mathbf{p}}, \tilde{\mathbf{q}})$ being similar, and we begin with the proof of (45, left). By definition of the quadratic function $\overline{U}$, one has for any $1 \le i \le d'$

$$\begin{aligned}&\max\{0, \overline{U}(\overline{\mathbf{p}})/\lambda - \overline{U}(\overline{\mathbf{p}} + \dot{\mathbf{e}}_i)/\lambda + h\langle\hat\eta(\overline{\mathbf{p}}), \dot{\mathbf{e}}_i\rangle,\ \overline{U}(\overline{\mathbf{p}})/\lambda - \overline{U}(\overline{\mathbf{p}} - \dot{\mathbf{e}}_i)/\lambda - h\langle\hat\eta(\overline{\mathbf{p}}), \dot{\mathbf{e}}_i\rangle\} \\ &= h|\langle\overline{\mathbf{w}}/\lambda - \hat\eta(\overline{\mathbf{p}}), \dot{\mathbf{e}}_i\rangle| + \frac{h^2}{\delta}\|\dot{\mathbf{e}}_i\|^2.\end{aligned} \tag{46}$$

From this point, the arguments developed in the Riemannian case apply without modification. The second estimate (45, right) follows from

$$\big|\|\overline{\mathbf{w}} - \hat\eta(\overline{\mathbf{q}})\|_{\mathcal{D}(\overline{\mathbf{q}})} - \|\overline{\mathbf{w}} - \hat\eta(\overline{\mathbf{p}})\|_{\mathcal{D}(\overline{\mathbf{p}})}\big| \le C^{\mathcal{D}}_{\mathrm{Lip}}\|\overline{\mathbf{p}} - \overline{\mathbf{q}}\|(\|\overline{\mathbf{w}}\| + \|\hat\eta(\overline{\mathbf{q}})\|) + \lambda^*(\mathcal{D})C^{\hat\eta}_{\mathrm{Lip}}\|\overline{\mathbf{p}} - \overline{\mathbf{q}}\|,$$

combined with $\|\overline{\mathbf{p}} - \overline{\mathbf{q}}\| \le 4C^u_{\mathrm{Lip}}\delta$, see Theorem 2.3, hence $\|\overline{\mathbf{w}}\| \le 4C^u_{\mathrm{Lip}}$. Combining the two estimates (31) with Lemma 4.2, and using the convexity of the norm, we obtain

$$1 + C_0 r_* \frac{h}{\delta} \ge \|\overline{\mathbf{w}}/\lambda - \hat\eta(\overline{\mathbf{p}})\|_{\mathcal{D}(\overline{\mathbf{p}})} \ge \|\overline{\mathbf{w}} - \hat\eta(\overline{\mathbf{p}})\|_{\mathcal{D}(\overline{\mathbf{p}})} + \frac{1/\lambda - 1}{\|\overline{\mathbf{w}} - \hat\eta(\overline{\mathbf{p}})\|_{\mathcal{D}(\overline{\mathbf{p}})}}\langle\overline{\mathbf{w}}, \mathcal{D}(\mathbf{p})(\overline{\mathbf{w}} - \hat\eta(\overline{\mathbf{p}}))\rangle$$

The scalar product in the above r.h.s. is bounded below as follows

$$\begin{aligned}2\langle\overline{\mathbf{w}}, \mathcal{D}(\mathbf{p})(\overline{\mathbf{w}} - \hat\eta(\overline{\mathbf{p}}))\rangle &= \|\overline{\mathbf{w}} - \hat\eta(\overline{\mathbf{p}})\|^2_{\mathcal{D}(\mathbf{p})} + \|\overline{\mathbf{w}}\|^2_{\mathcal{D}(\overline{\mathbf{p}})} - \|\hat\eta(\mathbf{p})\|^2_{\mathcal{D}(\mathbf{p})} \\ &\ge \|\overline{\mathbf{w}} - \hat\eta(\overline{\mathbf{p}})\|^2_{\mathcal{D}(\mathbf{p})} - (1 - c_{\mathcal{D},\eta})^2\end{aligned}$$

Using $\|\overline{\mathbf{w}} - \hat\eta(\overline{\mathbf{p}})\|_{\mathcal{D}(\mathbf{p})} \ge 1 - C_1\delta$, and assuming $2C_1\delta \le c_{\mathcal{D},\eta}$ for the second inequality, we obtain

$$1 + C_0 r_* \frac{h}{\delta} \ge (1 - C_1\delta) + (1/\lambda - 1)\left((1 - C_1\delta) - \frac{(1 - c_{\mathcal{D},\eta})^2}{1 - C_1\delta}\right) \ge (1 - C_1\delta) + (1 - \lambda)\frac{c_{\mathcal{D},\eta}}{2}.$$

We used the elementary inequalities $1/\lambda - 1 \ge 1 - \lambda$ and $(1 - c/2) - (1 - c)^2/(1 - c/2) \ge c/2$. This implies the announced lower bound for λ. □

Establishing assumption (ii) of Theorem 2.3. The case of Rander metrics only requires a minor adaptation of the Riemannian argument, presented Proposition 2.10.

Proposition 4.4. *Let $\mathbf{p} \in \Omega_h$, and let $\mathbf{q} \in \mathbb{E}$ be such that $\|\mathbf{p}-\mathbf{q}\| \geq C_0 r_* h$, where $C_0 := \mu(\mathcal{D})\sqrt{d'}$. Then there exists $1 \leq i \leq d'$ and a sign $s \in \{-1,1\}$ such that*

$$U_h(\mathbf{p}) \leq U_h(\mathbf{p} + hs\dot{\mathbf{e}}_i) + hC_1\|\dot{\mathbf{e}}_i\|, \qquad \|\mathbf{p} + hs\dot{\mathbf{e}}_i - \mathbf{q}\| \leq \|\mathbf{p}-\mathbf{q}\| - hc_2\|\dot{\mathbf{e}}_i\|,$$

with $C_1 := \lambda^*(\mathcal{M})\sqrt{d'} + \|\hat{\eta}\|_\infty$, $c_2 := 1/(2\mu(\mathcal{D})\sqrt{d'})$. This implies assumption (ii) of Theorem 2.3, with the constants $C^U_{\mathrm{bd}} = C_1/c_2$, $C'^U_{\mathrm{bd}} := C_{\mathrm{bd}} C_\Omega C_0 r_*$, and $c^U_{\mathrm{bd}} = +\infty$.

Proof. The arguments developed in the Riemannian case apply with the following adaptation of (36): by definition of the discretization scheme (43) one has $h^{-2}\rho^2 \max\{0, U_h(\mathbf{p}) - U_h(\mathbf{p}+\dot{\mathbf{e}}) - h\langle\hat{\eta}(\mathbf{p}), \dot{\mathbf{e}}\rangle\}^2 \leq (\mathfrak{F}_h U_h(\mathbf{p}))^2 = 1$, hence

$$U(\mathbf{p}) - U(\mathbf{p}+\dot{\mathbf{e}}) \leq \frac{h}{\rho} + h\langle\hat{\eta}(\mathbf{p}), \dot{\mathbf{e}}\rangle \leq h\|\dot{\mathbf{e}}\|(\frac{\sqrt{d'}}{\lambda_*} + \|\hat{\eta}\|_\infty). \qquad \square$$

5 Numerical results

We demonstrate the numerical methods introduced in this paper in a series of numerical experiments, involving Riemannian, sub-Riemannian and Rander metrics in §5.1, §5.2 and §5.3 respectively. Open source numerical codes for the Riemannian and sub-Riemannian models[1] are available on the author's webpage[2].

5.1 Riemannian examples

We validate our algorithm on a number of two and three dimensional test cases, which are split into two groups. The problems of the first group - related to differential geometry and seismic imaging - feature smooth Riemannian metrics with pronounced yet bounded anisotropy, and accuracy is the main concern. The problems of the second group - related to tubular structure segmentation in medical image data - feature discontinuous Riemannian metrics and extreme anisotropies, and robustness is the main concern.

Smooth Riemannian metrics. The first test, two dimensional and introduced in [36], is the computation of the distance from the origin w.r.t. the riemannian metric induced on a parametric surface by the euclidean metric on $\mathbb{R}^3$. The surface is described by the height map

$$z(x,y) := (3/4)\sin(3\pi x)\sin(3\pi y),$$

hence the Riemannian metric is $\mathcal{M}(x,y) = \mathrm{Id} + \nabla z(x,y) \nabla z(x,y)^{\mathrm{T}}$, which maximum condition number (4) is ≈ 5.1. The parametrization domain, is the unit square $[-0.5, 0.5]^2$ rotated by the angle $\pi/6$.

The second test, two dimensional and introduced in [30], is inspired by seismic imaging applications. The Riemannian metric tensor $\mathcal{M}(x,y)$ has eigenvector $(1, (\pi/2)\cos(4\pi x))$ with eigenvalue 0.8^{-2}. The second eigenvalue is 0.2^{-2}, hence the condition number is 4. The parametrization domain is $[-0.5, 0.5]^2$, and the distance is computed from the origin.

[1] Numerical codes for Rander metrics, which are more experimental, are available on demand.

[2] `https://github.com/Mirebeau`

The third test, introduced here for the first time, extends the seismic imaging inspired second test to three dimensions. The Riemannian metric tensor $\mathcal{M}(x, y, z)$ has eigenvector $(\cos(3\pi(x + y)), \sin(3\pi(2x - y)), 0.5)$, with eigenvalue 0.2^{-2}. The two other eigenvalues are equal to 0.8^{-2}, hence the condition number is 4. The domain is $[-0.5, 0.5]^3$ and the distance is computed from the origin $(0, 0, 0)$.

Numerical results for these three tests are presented in Figure 3. The accuracy and computation time in the two dimensional test cases are compared in Appendix §B with several alternative numerical methods. The proposed method is state of the art, comparable with the FM-LBR [18] but with the advantage of being compatible with second order finite differences.

Discontinuous Riemannian metrics with extreme anisotropy. Anisotropic fast marching methods have shown their relevance for image segmentation methods based on minimal paths [4, 8]. In these applications, the metric often varies quickly, if not discontinuously, both in orientation and aspect ratio. For instance, the Riemannian metric is often designed to favor paths which remain close and tangent to a collection of thin tubular structures in the image.

We present two numerical experiments inspired by these applications, in two and three dimensions respectively, which first appeared in [4] and [18]. The Riemannian metric is euclidean (identity matrix) except in the neighborhood of a curve Γ embedded in the domain, where the metric is extremely anisotropic, with eigenvalues $(1, 1/100^2)$ or $(1, 1, 1/50^2)$ in the two and three dimensional experiments, and the curve tangent vector Γ' is an eigenvector for the small eigenvalue. See Figure 4 for an illustration, and [18] for a complete description of the test cases.

Again the CPU time and accuracy of the FM-VR1 are state of the art, and comparable to those of the FM-LBR. In contrast, iterative numerical methods such as the AGSI [5], and fast marching methods based on less sophisticated stencil constructions [1], have be shown to fail on these types of benchmarks [4, 18]

5.2 Sub-riemannian models

We consider several sub-Riemannian models, posed on the domain $\mathbb{M} := \mathbb{R}^d \times \mathbb{S}^{d-1}$, which elements are denoted $\mathbf{p} = (\mathbf{x}, \mathbf{n})$, and tangent vectors $\dot{\mathbf{p}} = (\dot{\mathbf{x}}, \dot{\mathbf{n}})$. For that purpose, let us introduce the orthogonal projection

$$P_{\mathbf{n}}(\dot{\mathbf{x}}) := \dot{\mathbf{x}} - \langle \mathbf{n}, \dot{\mathbf{x}} \rangle \mathbf{n}$$

of a vector $\dot{\mathbf{x}}$ onto the hyperplane orthogonal to a given unit vector $\mathbf{n} \in \mathbb{S}^{d-1}$. We choose to describe the sub-Riemannian models via the relaxed Riemannian metric $\mathcal{M}_\varepsilon$, which is often easier to read than the control vector fields $(\omega_i)_{i=1}^n$ or the dual tensors $\mathcal{D}_\varepsilon$.

Reeds-Shepp model. The first considered model is the Reeds- Shepp subRiemannian model, with relaxed metric

$$\|\dot{\mathbf{p}}\|^2_{\mathcal{M}_\varepsilon(\mathbf{p})} := \mathcal{S}(\mathbf{p})^{-2} \left(\langle \mathbf{n}, \dot{\mathbf{x}} \rangle^2 + \varepsilon^{-2} \|P_{\mathbf{n}}(\dot{\mathbf{x}})\|^2 + \xi^2 \|\dot{\mathbf{n}}\|^2 \right) \tag{47}$$

where $\mathcal{S} : \mathbb{M} \to]0, \infty[$ is a point dependent speed function, with physical units [length]/[time], and ξ is a parameter which has the dimension [length] of a radius of curvature. Note that the choice of speed function $\mathcal{S}$ is typically application dependent and data driven, and that there is no obstruction, theoretical or practical, to letting ξ depend on the current point $\mathbf{p} \in \mathbb{M}$. This model is related to curvature penalization for the following reason: consider a smooth path $\mathbf{x} : [0, T] \to \mathbb{R}^d$, with non-vanishing speed. Then there exists a unique $\mathbf{n} : [0, T] \to \mathbb{S}^{d-1}$ such

that the lifted path $t \in [0,T] \mapsto \gamma(t) = (\mathbf{x}(t), \mathbf{n}(t))$ has finite length with respect to the sub-Riemannian metric $\mathcal{M}_0$. Indeed, one must set $\mathbf{n}(t) := \dot{\mathbf{x}}(t)/\|\dot{\mathbf{x}}(t)\|$, so that $P_{\mathbf{n}(t)}(\dot{\mathbf{x}}(t)) = 0$ for all $t \in [0,T]$. Then denoting by $\kappa(t) := \|\dot{\mathbf{n}}(t)\|/\|\dot{\mathbf{x}}(t)\|$ the curvature of the path $\mathbf{x}$ one obtains

$$\int_0^T \|\dot{\gamma}(t)\|_{\mathcal{M}_0(t)} \, \mathrm{d}t = \int_0^T \sqrt{1 + \xi^2 \kappa(t)^2} \, \frac{\|\dot{\mathbf{x}}(t)\| \, \mathrm{d}t}{\mathcal{S}(\gamma(t))}.$$

Note that (contrary to what this discussion may suggest) the physical projections of geodesics paths for the sub-Riemannian metric $\mathcal{M}_0$ are only piecewise smooth, because they generically feature *cusps*, see Figures 5, 7, and the discussion in [12].

Some experiments involving two and three dimensional physical paths are presented in Figures 5, 6 and 7. We are here solving strongly anisotropic PDEs on three and five dimensional domains respectively. The control sets for the Reeds-Shepp model posed on $\mathbb{R}^2 \times \mathbb{S}^1$ are illustrated on Figure 2 (ii). For the model posed on $\mathbb{R}^3 \times \mathbb{S}^2$, the sphere $\mathbb{S}^2$ is parametrized using the Euler angles $(\theta, \varphi) \mapsto (\cos\theta, \sin\theta\cos\varphi, \sin\theta\sin\varphi)$, from the flat domain $[0,\pi] \times [0, 2\pi]$ equipped with the adequate Riemannian metric and boundary conditions.

The numerical results are similar to those obtained in [12] using the semi-lagrangian FM-LBR, but computation times are substantially smaller for the 5D test case, see the discussion in §5.1, by a factor 5 typically for the five dimensional test cases.

A model related to torsion penalization. We introduce a new sub-Riemannian model, which relaxed metric is defined for all $\mathbf{p} = (\mathbf{x}, \mathbf{n}) \in \mathbb{M}$, $\dot{\mathbf{p}} = (\dot{\mathbf{x}}, \dot{\mathbf{n}}) \in T_{\mathbf{p}}\mathbb{M}$ by

$$\|\dot{\mathbf{p}}\|^2_{\widetilde{\mathcal{M}}_\varepsilon(\mathbf{p})} := \mathcal{S}(\mathbf{p})^{-2} \left(\langle \mathbf{n}, \dot{\mathbf{x}} \rangle^2 + \varepsilon^{-2} \|P_{\mathbf{n}}(\dot{\mathbf{x}})\|^2 + \xi^2 \|\dot{\mathbf{n}}\|^2 \right), \tag{48}$$

where again $\mathcal{S} : \mathbb{M} \to]0, \infty[$ is the speed function, and ξ has the dimension of a length. The model (48) favors *planar* paths, which was the motivation of torsion penalization in the first place [33]. Indeed the physical velocity $\dot{\mathbf{x}}$ is constrained by the cost of $\varepsilon^{-2}\langle \mathbf{n}, \dot{\mathbf{x}} \rangle^2$ to remain (approximatedly if $\varepsilon > 0$) in the plane orthogonal to the vector $\mathbf{n}$, which variation is itself controlled by the cost of $\|\dot{\mathbf{n}}\|^2$. Note also that the most natural way to lift a physical curve $\mathbf{x} : [0,T] \to \mathbb{R}^3$ into $\gamma = (\mathbf{x}, \mathbf{n}) : [0,T] \to \mathbb{R}^3 \times \mathbb{S}^2$ obeying the orthogonality constraint $\langle \mathbf{x}(t), \mathbf{n}(t) \rangle = 0$ for all $t \in [0,T]$, is to define $\mathbf{n}(t) := (\dot{\mathbf{x}}(t) \times \ddot{\mathbf{x}}(t))/\|\dot{\mathbf{x}}(t) \times \ddot{\mathbf{x}}(t)\|$. Then denoting by $\tau(t) := \|\dot{\mathbf{n}}(t)\|/\|\dot{\mathbf{x}}(t)\|$ the torsion of the path $\mathbf{x}$ one obtains

$$\int_0^T \|\dot{\gamma}(t)\|_{\widetilde{\mathcal{M}}_0(t)} \, \mathrm{d}t = \int_0^T \sqrt{1 + \xi^2 \tau(t)^2} \, \frac{\|\dot{\mathbf{x}}(t)\| \, \mathrm{d}t}{\mathcal{S}(\gamma(t))}.$$

Nevertheless our model is only related to torsion penalization, and not equivalent to it, because there exists other lifts $\gamma = (\mathbf{x}, \mathbf{n}) : [0,T] \to \mathbb{R}^d \times \mathbb{S}^{d-1}$ of the curve $\mathbf{x} : [0,T] \to \mathbb{R}^d$ obeying the required orthogonality constraint, and which energy could be smaller than the torsion based one.

Numerical experiments presented in Figures 6 and 7 show that the orthogonality relation $\langle \mathbf{n}(t), \dot{\mathbf{x}}(t) \rangle = 0$ is indeed approximately satisfied by the extracted paths. On the experiment presented Figure 6, the speed function $\mathcal{S} : \mathbb{R}^3 \times \mathbb{S}^2 \to]0, \infty[$ only depends on the physical position $\mathbf{x}$, and is small away from two curves Γ_1, Γ_2 of interest

$$\mathcal{S}(\mathbf{x}, \mathbf{n}) := \max\{s, \exp\left(-\frac{\mathrm{dist}(\mathbf{x}, \Gamma_1 \cup \Gamma_2)^2}{2\sigma^2} \right)\},$$

where $s = 1/6$ and $\sigma = 0.15$. The curves Γ_1, Γ_2 are parametrized by $t \in [0, \pi]$ as follows

$$\gamma_1(t) := (t, \sin(t)^2 \cos(4t), 0), \qquad \gamma_2(t) := (t, \sin(t)^3 \cos(2t), \sin(t)^3 \sin(2t)).$$

Hence Γ_1 has large curvature but no torsion, whereas Γ_2 has small curvature but some torsion. Using our anisotropic fast marching method, we compute the shortest path between the common endpoints $\mathbf{x}_0, \mathbf{x}_1 \in \mathbb{R}^3$ of these curves, among all possible orientations of the unit vector $\mathbf{n}_0, \mathbf{n}_1 \in \mathbb{S}^2$. As could be expected, the torsion related model selects a path along Γ_1, whereas the Reeds-Shepp model selects a path along Γ_2.

On Figure 6 we validate our sub-Riemannian fast marching method by comparing the obtained minimal paths with solutions of the Hamilton equations of geodesics

$$\frac{d\mathbf{p}}{dt} = -\frac{\partial \mathcal{H}}{\partial \hat{\mathbf{p}}} \qquad\qquad \frac{d\hat{\mathbf{p}}}{dt} = \frac{\partial \mathcal{H}}{\partial \hat{\mathbf{p}}}, \tag{49}$$

where $\mathcal{H}(\mathbf{p}, \hat{\mathbf{p}}) := \frac{1}{2}\langle \hat{\mathbf{p}}, \mathcal{D}_0(\mathbf{p})\hat{\mathbf{p}}\rangle$. We denoted by $\mathcal{D}_0$ the inverse tensor to the sub-Riemannian metric (47) (resp. (48)), which is well defined in contrast to $\mathcal{M}_0$ itself. The ODE is solved using a fourth order Runge-Kutta method, and the ODE initial conditions are adjusted using a Newton method to match the desired endpoints.

5.3 Rander models

We consider some instances of Zermelo's navigation problem, which models vehicles such as planes or boats moving within a domain $\Omega \subseteq \mathbb{R}^d$ and subject to a given drift $\dot{\eta} : \overline{\Omega} \to \mathbb{R}^d$. The objective is to find the minimal time $T \geq 0$ for which there exists a path $\gamma : [0, T] \to \overline{\Omega}$, connecting two given points $\gamma(0) = \mathbf{p}_0, \gamma(1) = \mathbf{p}_1 \in \overline{\Omega}$, and subject for all $t \in [0, T]$ to the constraint

$$\|\dot{\gamma}(t) - \dot{v}(\gamma(t))\| \leq 1.$$

We present a two and a three dimensional experiment, on the domains $\Omega = [0, 1]^2$ and $\Omega = [0, 1]^3$. The drift has the explicit expression

$$\dot{\eta}(\mathbf{x}) := \alpha \sin(4\pi \mathbf{x}_1)\sin(4\pi \mathbf{x}_2)\frac{\mathbf{x}}{\|\mathbf{x}\|}. \quad \Big(\text{resp. } \dot{\eta}(\mathbf{x}) := \alpha \sin(4\pi \mathbf{x}_1)\sin(4\pi \mathbf{x}_2)\sin(4\pi \mathbf{x}_3)\frac{\mathbf{x}}{\|\mathbf{x}\|}.\Big)$$

The two dimensional instance was first presented in [30]. Note that $\|\dot{\eta}(\mathbf{x})\| < 1$ for all $\mathbf{x} \in \mathbb{R}^d$, otherwise the system would not be locally controllable, and the proposed method would not be applicable. The PDE solved is

$$\|\mathrm{d}u(\mathbf{p}) - \hat{\eta}(\mathbf{p})\|_{\mathcal{D}(\mathbf{p})} = 1,$$

where, as follows from Proposition 1.13 and expression of the dual to a Rander metric given in [17],

$$\mathcal{D}(\mathbf{p}) := (1 - \|\dot{v}(\mathbf{p})\|^2)(1 - \dot{v}(\mathbf{p}) \otimes \dot{v}(\mathbf{p})), \qquad\qquad \hat{\eta}(\mathbf{p}) = \frac{-\dot{\eta}(\mathbf{p})}{1 - \|\dot{\eta}(\mathbf{p})\|^2}.$$

Since the resulting numerical scheme lacks the causality property, see Definition 2.1, the fast marching method is not applicable. We use instead Adaptive Gauss Siedel Iterations, in the spirit of [5].

The computation time and the L^∞ and L^1 errors obtained with the two dimensional problem are presented in §B, and compared with several alternative semi-lagrangian methods [17, 5, 1]. In summary, the proposed method works well but does not outperform its alternatives on this test case, in particular Fast Marching using Anisotropic Stencil Refinement (FM-ASR) [17]. The following points are however in defense of the the discretization introduced in this paper:

- (Dimension) The proposed discretization applied in arbitrary dimension, whereas the stencil construction of the FM-ASR is intrinsically two dimensional.

- (Second order accuracy) The proposed discretization can take advantage of second order finite differences to improve accuracy by one order of magnitude or more, as demonstrated in §B, in contrast with the semi-lagrangian methods.

6 Conclusion

In this paper, we introduced a new discretization of anisotropic eikonal equations on cartesian grids. The discretization makes use of adaptive stencils built using a tool from discrete geometry: Voronoi's first reduction of quadratic forms.

Convergence proof is provided, with convergence rates, is the setting of riemannian metrics, but also sub-riemannian and asymmetric Rander metrics. Numerical experiments show that the method is particularly suitable for problems with one or more of the following features: (i) strong anisotropy, with Riemannian tensor condition numbers of ≈ 10 and more, (ii) high dimension, up to 5, (iii) high accuracy requirements, addressed using second order finite differences.

Future directions of research include (a) causal discretizations for non-symmetric Hamiltonians, (b) point sets more general than cartesian grids, either unstructured or obtained by gluing several grid patches of different scales, (c) applications to motion planning and image segmentation.

Acknowledgement. The author thanks Jorg Portegies, PhD student at Eindhoven TU/e University under the direction of Remco Duits, for careful testing of the numerical codes and designing some of the numerical experiments.

A Figures for the numerical experiments

B Two dimensional benchmark

We compare the accuracy and computation time of the proposed algorithm with several alternative methods proposed in the literature. They can be divided into two groups: causal discretizations, solved via the single pass fast marching algorithm, and non-causal discretizations, solved via iterative methods. These groups are analogous, in the context of distance computation on graphs, to Dijkstra's algorithm and Bellman-Ford's algorithm respectively, and the counterpart of causality is the positivity of the edge weights.

Our numerical tests confirm the good performance discretization introduced in this paper, which does not outperform [17, 18], but compensates for this by its compatibility with second order finite differences, its generalization potential, and its CPU time advantage in the high dimensional problems §5.2. This benchmark extends previous works of the author published in [17, 18].

Causal discretizations.

- Fast Marching using Voronoi's first reduction (FM-VR1), introduced in this paper.
- Fast-Marching using Lattice Basis Reduction (FM-LBR), and Fast-Marching using Adaptive Stencil Refinement (FM-ASR), introduced by the author in [18] and [17]. Like the FM-VR1, these are a single pass methods, which require a cartesian grid, and achieve their efficiency by the use of adaptive stencils built using arithmetic techniques. In contrast with the FM-VR1, these are semi-Lagrangian discretizations. FM-LBR is intended

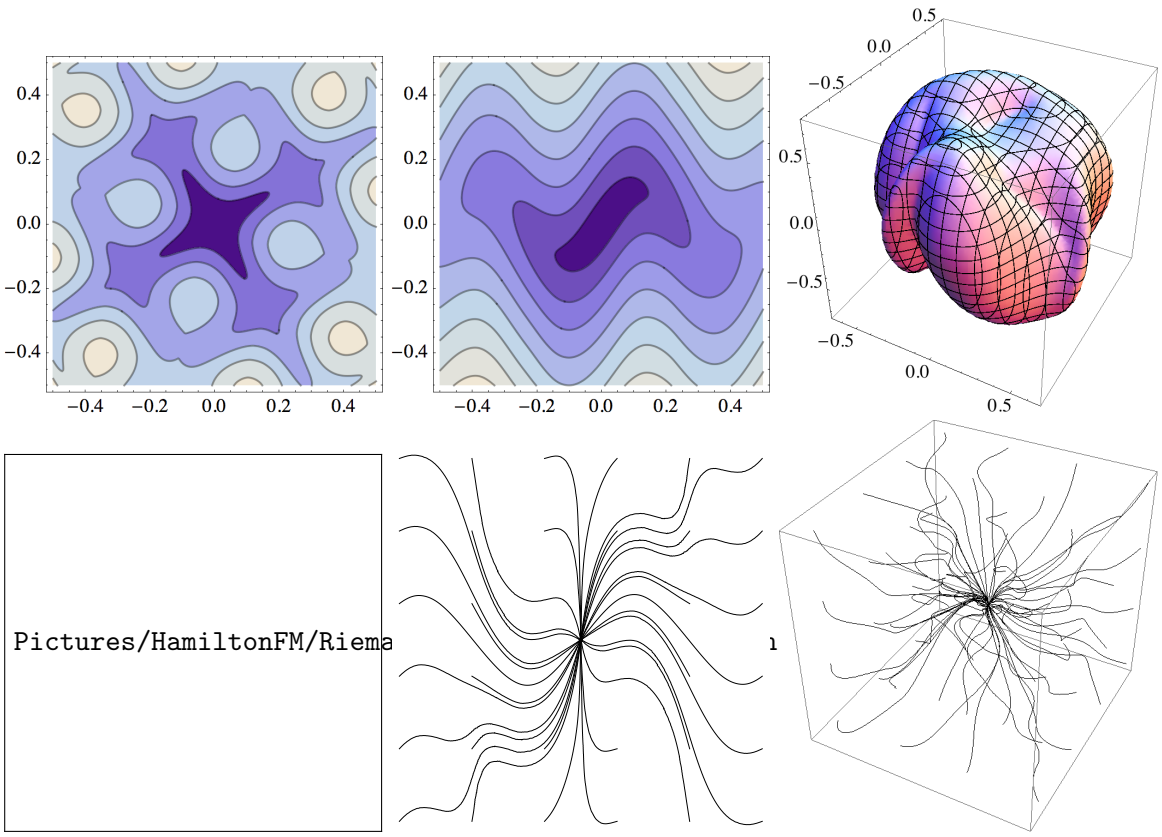

Figure 3: Numerics for smooth Riemannian metrics, illustrating §5.1. Test cases involving smooth riemannian metrics. Top: level lines of the distance maps. Bottom: some minimal geodesics. Left: distance computation on a parametric surface, 283^2 grid, 0.1s CPU time. Center: inspired by seismic data analysis, 193^2 grid, 0.04s CPU time. Right: likewise in 3D, on a 101^3 grid, CPU time 5.02s. See Appendix B for more CPU information and accuracy comparisions.

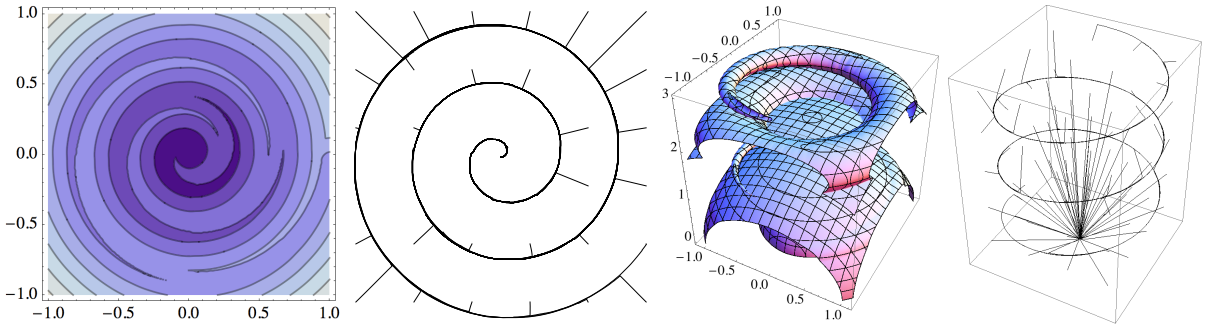

Figure 4: Numerics for discontinuous, extremely anisotropic Riemannian metrics, illustrating §5.1. Test cases inspired by tubular structure segmentation, favoring paths which remain close and tangent to a curve, featuring discontinuous and extremely anisotropic Riemannian metrics. Left: 201×201 grid, 0.03s CPU time. Right $201 \times 201 \times 272$ grid, 25s CPU time.

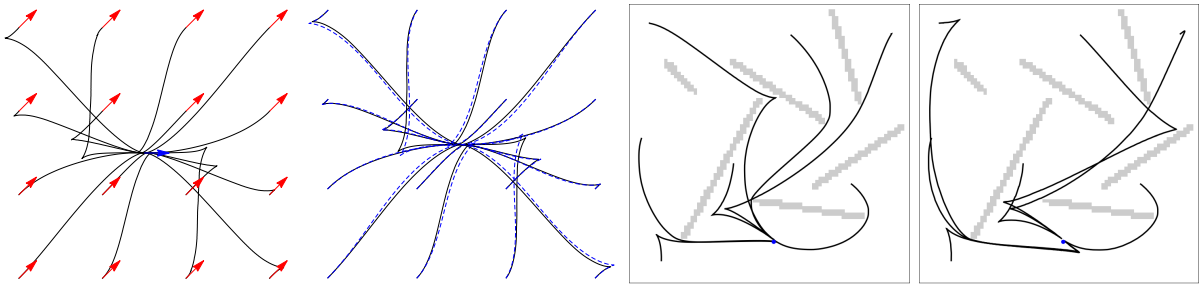

Figure 5: Numerics for the Reeds-Shepp sub-Riemannian model posed on $\mathbb{R}^2 \times \mathbb{S}^1$, illustrating §5.2. Left: minimal paths without obstacles, model parameters $\varepsilon = 0.1$, $\xi = 0.3$. Center left: likewise, with dashed lines obtained using an ODE shooting method based on the Hamilton equations of geodesics. Center right and right: Path planning with the Reeds-Shepp model in the presence of obstacles. Domain $[0,1]^2 \times \mathbb{S}^1$ discretized on a $90^2 \times 60$ grid, CPU time 0.36s. Model parameters $\varepsilon = 0.1$, and $\xi = 0.4$ or 0.8 respectively.

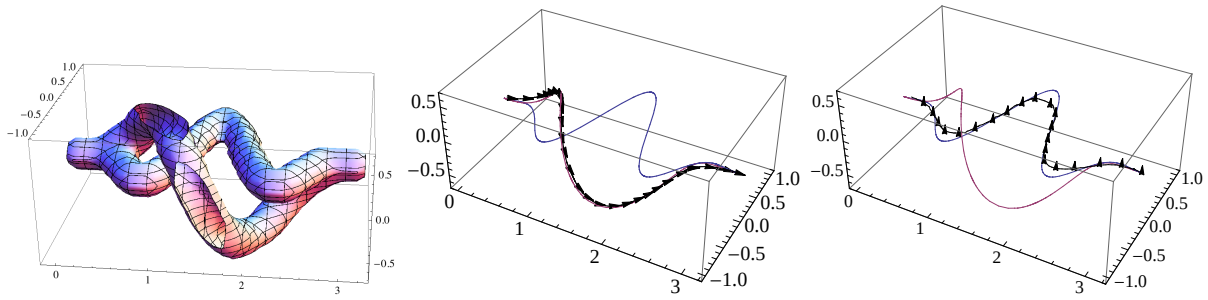

Figure 6: Numerics for sub-riemannian models posed on $\mathbb{R}^3 \times \mathbb{S}^2$, illustrating §5.2. Test case inspired by 3D tubular structure segmentation. Left: contour plot of the speed function, which is high in the neighborhood of two curves of small curvature and small torsion respectively. The curvature-penalized model (center) and the torsion-penalized-like model (right) select distinct paths. Domain $([0,\pi] \times [-1,1] \times [-1,0.5]) \times \mathbb{P}^2$ discretized using a $(40 \times 20 \times 16) \times (5 \times 20)$ grid, $\varepsilon = 0.2$. CPU time 6.6 s.

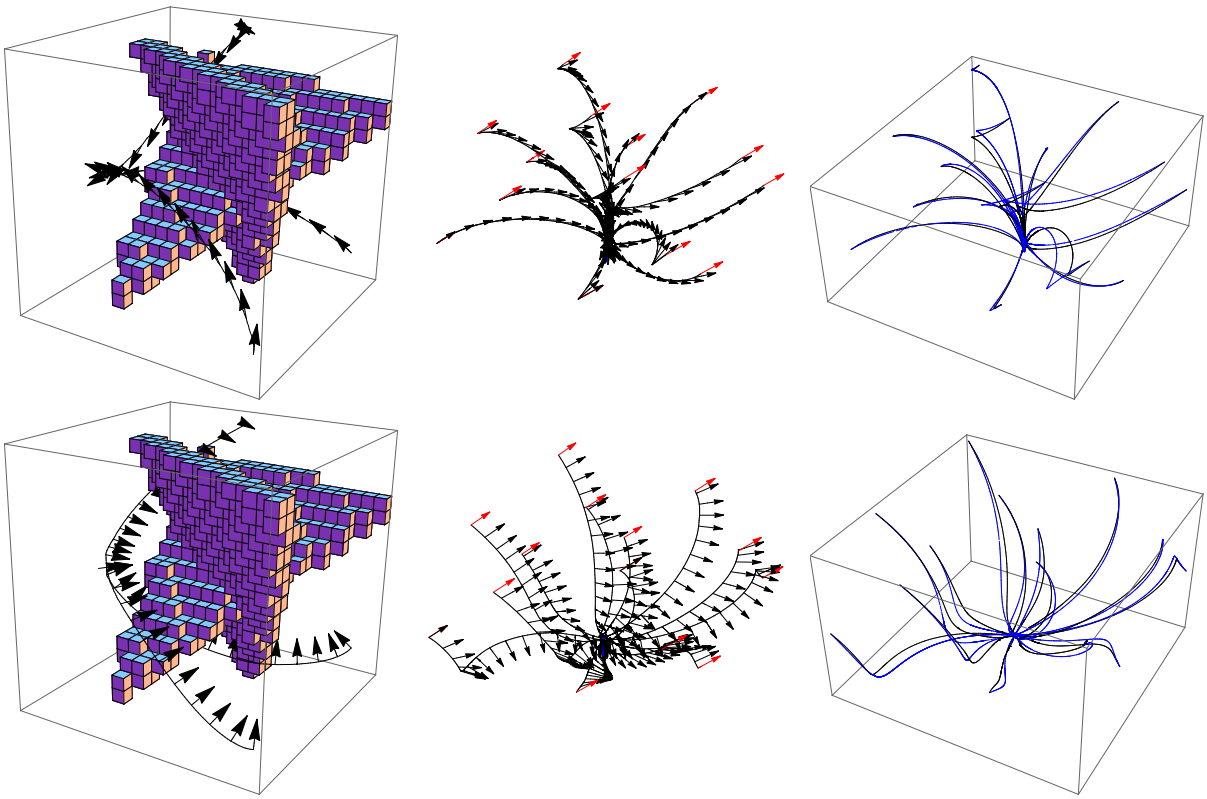

Figure 7: Numerics for sub-riemannian models posed on $\mathbb{R}^3 \times \mathbb{S}^2$, illustrating §5.2. Top: curvature-penalized model. Bottom: torsion-penalized-like model. Left: minimal paths in the presence of obstacles. $\xi = 0.2$, domain $[0,1]^3 \times \mathbb{P}^2$. Size $20^3 \times (5 \times 20)$, $\varepsilon = 0.2$. CPU time 2.6s and 2.4s. Center: Minimal paths with constant cost, $\varepsilon = 0.1$, $\xi = 0.5$. The vector $\mathbf{n}(t)$, illustrated with arrows, satisfies approximatedly as required the sub-riemannian constraint $\mathbf{n}(t) \times \dot{\mathbf{x}}(t) = 0$ (top) or $\langle \mathbf{n}(t), \dot{\mathbf{x}}(t) \rangle = 0$ (bottom). Right: comparison with an ODE shooting method based on Hamilton's equations of geodesics.

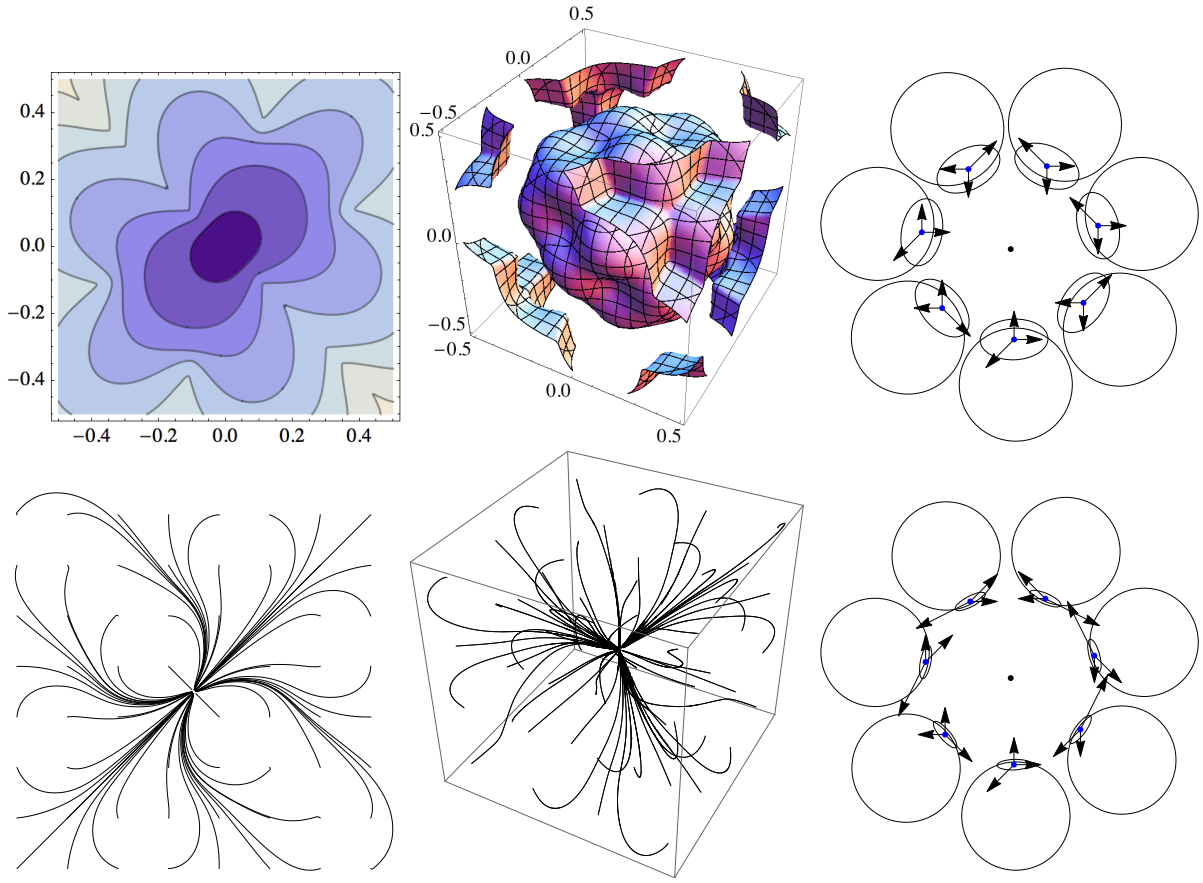

Figure 8: Numerics for Rander metrics, Illustrating §5.3. Left: Two dimensional instance of Zermelo's navigation problem. Metric etric anisotropy ratio 19, 201×201 grid, 0.14s CPU time. Level lines of the solution (top) and some geodesics (bottom) Center: Likewise in three dimensions. Grid size 101^3, CPU time 7.8s. Right examples of non-centered control sets, and stencils used in the discretization.

	FM-VR1					
	1st order	2nd order	FM-LBR	FM-8	FE	MAOUM
	Embedded surface distance test, 293×293 grid					
CPU time	0.10*	0.12*	0.20	0.21	1.44	1.31
L^∞ error	5.8	1.2**	5.52	12.5	9.45	8.56
L^1 error	1.6	0.063	1.46	3.42	2.51	2.52
	Seismic inspired test, 193×193 grid					
CPU time	0.042*	0.048*	0.076	0.079	0.77	0.36
L^∞ error	4.5	0.26**	2.90	3.03	3.67	7.66
L^1 error	1.5	0.052	1.03	1.30	1.40	2.3

Figure 9: Comparison of the CPU time and accuracy of the proposed FM-VR1 with several alternatives in two Riemannian test cases, see §5.1 and §B. All errors multiplied by 100 for readability. When testing second order accuracy, the seed point $(0, 0)$ was replaced with a precomputed solution on the disk $D(0, 1/8)$. Asterix * a slightly faster CPU was used for the new tests (2.7GHz instead of 2.4GHz). Asterix ** a layer of 5 pixels along the domain boundary was excluded.

	RD-VR1					
	1st order	2nd order	FM-ASR	FM-8	FE	MAOUM
	Zermelo navigation problem, 285×285 grid					
CPU time	1.03(0.48*)	1.39(0.81*)	0.29	0.16	1.08	0.69
L^∞ error	0.74	0.20	0.64	0.64	1.05	2.8
L^1 error	0.38	0.01	0.13	0.11	0.41	0.17

Figure 10: Comparison of the CPU times and accuracy of the proposed RD-VR1 method with several alternatives in a test case involving a Rander metric, see §5.3 and §B. All errors multiplied by 100 for readability. When testing second order accuracy, the single seed point was replaced with an accurate precomputed solution within the subdomain $[-1/10, 1/10]^2$. Asterix * first time using the AGSI as decribed in [5], second time with a variant which limits the front width to 10 pixels.

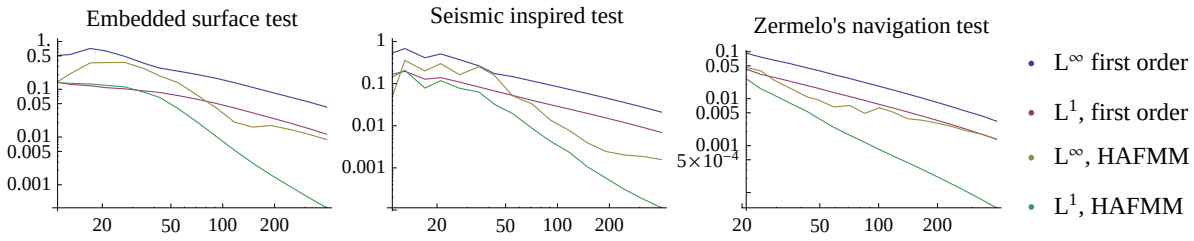

Figure 11: Numerical error as a function of gridsize for the two dimensional test cases. Second order convergence is achieved in the L^1 norm, but not in the L^∞ norm (despite the removal of a 5 pixel layer along the boundary), which is not surprising since solutions to eikonal equations are not smooth along a $(d-1)$-dimensional interface called the cut locus.

for two and three dimensional Riemannian metrics, and FM-ASR for two dimensional Finslerian metrics.

- The Monotone Acceptance Ordered Upwind method (MAOUM) [1] is a single pass semi-Lagrangian method using adaptive stencils. It differs from the FM-LBR and FM-ASR by its less sophisticated stencil construction, which produces large isotropic stencils, often at the expense of accuracy and complexity.

- Fast-Marching using 8-point stencils (FM-8) is the original semi-Lagrangian scheme [34] instantiated with non-adaptive 8-point stencils. This method is *non-consistent* for Riemannian metrics which condition number exceeds $1 + \sqrt{2}$, because its stencils lack the acuteness property [29]. Hence convergence towards the continuous problem solution *fails* as the grid is refined. Nevertheless, the method is fast and its accuracy is surprisingly competitive at low grid sizes.

Non causal discretizations. We use Adaptive Gauss Siedel Iterations (AGSI[3]) to solve the following discretizations. We also report some computation times obtained with a variant of this method limiting the front width to 10 pixels.

- Rander Distances using Voronoi's First Reduction (RD-VR1), introduced in this paper.

- The Finite Element discretization (FE) of [5], a semi-Lagrangian discretization using non-adaptive stencils extracted from a triangulation of the domain, here by half-squares.

All CPU times obtained using a single thread. CPU times are empirical data, only indicative of general performance. CPU times for the FM-VR1 and RD-VR1 obtained on a 2.7GHz core i7 laptop, whereas CPU times for the other methods were copied from previous works [18, 17] and obtained using a 2.4 GHz core 2 duo laptop.

C Doubling of variables

We establish in this section the doubling of variables argument, presented in Theorem 2.3 and adapted from [13]. Since the domain Ω is by assumption bounded, its closure $\overline{\Omega}$ is compact, and its sampling $\Omega_h := \Omega \cap h\mathbb{L}$ is finite. Since the functions u and U_h are supported on these sets, and since u is C_{Lip}-Lipschitz hence continuous, the maxima $\overline{M}_{\lambda,\delta}$ and $\widetilde{M}_{\lambda,\delta}$ are well defined and attained, at some point pairs $(\overline{\mathbf{p}}, \overline{\mathbf{q}}), (\tilde{\mathbf{p}}, \tilde{\mathbf{q}}) \in (h\mathbb{L}) \times \mathbb{E}$. Our first step is to establish the closeness of $\overline{\mathbf{p}}$ with $\overline{\mathbf{q}}$, and of $\tilde{\mathbf{p}}$ with $\tilde{\mathbf{q}}$, as announced in Theorem 2.3.

Lemma C.1. *Under the assumptions of Theorem 2.3, one has* $\max\{\|\overline{\mathbf{p}}-\overline{\mathbf{q}}\|, \|\tilde{\mathbf{p}}-\tilde{\mathbf{q}}\|\} \leq 4C_{\text{Lip}}\delta$.

Proof. Using the optimality properties defining $(\overline{\mathbf{p}}, \overline{\mathbf{q}})$ and $(\tilde{\mathbf{p}}, \tilde{\mathbf{q}})$, see Theorem 2.3, and comparing with the alternative point pairs $(\overline{\mathbf{p}}, \overline{\mathbf{p}})$ and $(\tilde{\mathbf{p}}, \tilde{\mathbf{p}})$ respectively, one obtains

$$\lambda U_h(\overline{\mathbf{p}}) - u(\overline{\mathbf{q}}) - \frac{1}{2\delta}\|\overline{\mathbf{p}} - \overline{\mathbf{q}}\|^2 = \overline{M}_{\lambda,\delta} \geq \lambda U_h(\overline{\mathbf{p}}) - u(\overline{\mathbf{p}}),$$
$$\lambda u(\tilde{\mathbf{q}}) - U_h(\tilde{\mathbf{p}}) - \frac{1}{2\delta}\|\tilde{\mathbf{p}} - \tilde{\mathbf{q}}\|^2 = \widetilde{M}_{\lambda,\delta} \geq \lambda u(\tilde{\mathbf{p}}) - U_h(\tilde{\mathbf{p}}).$$

[3]Note that in [18, 17] the acronym AGSI refers to discretization FE of [5]. This is inadequate, since it mixes the PDE discretization and the numerical solver used for the discrete system of equations.

The next line is obtained by first rearranging the terms of these inequalities, eliminating in particular the instances of U_h, and then using the Lipschitz regularity of u

$$\frac{1}{2\delta}\|\overline{\mathbf{p}}-\overline{\mathbf{q}}\|^2 \le u(\overline{\mathbf{p}})-u(\overline{\mathbf{q}}) \le C_{\mathrm{Lip}}\|\overline{\mathbf{p}}-\overline{\mathbf{q}}\|, \quad \frac{1}{2\delta}\|\tilde{\mathbf{p}}-\tilde{\mathbf{q}}\|^2 \le \lambda(u(\tilde{\mathbf{q}})-u(\tilde{\mathbf{p}})) \le \lambda C_{\mathrm{Lip}}\|\tilde{\mathbf{q}}-\tilde{\mathbf{p}}\|.$$

The announced result follows from these estimates and the upper bound $1/\lambda \le 2$. □

The rest of this section is devoted to the proof of (25), and begins with an estimate of $u-U_h$ in terms of the suprema $\overline{M}_{\lambda,\delta}$, $\widetilde{M}_{\lambda,\delta}$ and of the max norm $\|u\|_\infty := \sup_{\mathbb{E}}|u|$, which is well defined by continuity of u and compactness of its support.

Lemma C.2. *Under the assumptions of Theorem 2.3, one has*

$$\sup_{\mathbf{p}\in h\mathbb{L}} |u(\mathbf{p})-U_h(\mathbf{p})| \le 2\left(\max\{\overline{M}_{\lambda,\delta},\widetilde{M}_{\lambda,\delta}\}+(1-\lambda)\|u\|_\infty\right).$$

Proof. By the optimality properties of $(\overline{\mathbf{p}},\overline{\mathbf{q}})$ and $(\tilde{\mathbf{p}},\tilde{\mathbf{q}})$ one obtains for any $\mathbf{p}\in\Omega_h$, respectively,

$$\overline{M}_{\lambda,\delta} \ge \lambda U_h(\mathbf{p})-u(\mathbf{p}) \ge \lambda(U_h(\mathbf{p})-u(\mathbf{p}))-(1-\lambda)\|u\|_\infty.$$
$$\widetilde{M}_{\lambda,\delta} \ge \lambda u(\mathbf{p})-U_h(\mathbf{p}) \ge (u(\mathbf{p})-U_h(\mathbf{p}))-(1-\lambda)\|u\|_\infty.$$

The announced result follows from these one-sided estimates on $u-U_h$, and from $1/\lambda\le 2$. □

The next paragraph establishes some conditional estimates on $\overline{M}_{\lambda,\delta}$ and $\widetilde{M}_{\lambda,\delta}$, depending on the location of the points $\overline{\mathbf{p}},\overline{\mathbf{q}},\tilde{\mathbf{p}},\tilde{\mathbf{q}}$. If $\tilde{\mathbf{p}}\in h\mathbb{L}\setminus\Omega_h$, then $U_h(\tilde{\mathbf{p}})=0$ and we obtain

$$\widetilde{M}_{\lambda,\delta} = \lambda u(\tilde{\mathbf{q}})-\frac{1}{2\delta}\|\tilde{\mathbf{p}}-\tilde{\mathbf{q}}\|^2 \le \lambda u(\tilde{\mathbf{q}}) \le \lambda C_{\mathrm{Lip}} d_{\partial\Omega}(\tilde{\mathbf{q}}) \le C_{\mathrm{Lip}}\|\tilde{\mathbf{p}}-\tilde{\mathbf{q}}\| \le 4C_{\mathrm{Lip}}^2\delta. \tag{50}$$

We used successively the negativity of the quadratic term, the Lipschitz regularity of u and the fact that it vanishes outside Ω, the fact that $\tilde{\mathbf{p}}\in h\mathbb{L}\setminus\Omega_h\subseteq\mathbb{E}\setminus\Omega$, and the previously obtained estimate on $\tilde{\mathbf{p}}-\tilde{\mathbf{q}}$. Likewise, if $\overline{\mathbf{p}}\in h\mathbb{L}\setminus\Omega_h$ then $\overline{M}_{\lambda,\delta}\le -u(\overline{\mathbf{p}})\le 4C_{\mathrm{Lip}}^2\delta$.

Next if $\overline{\mathbf{q}}\in\mathbb{E}\setminus\Omega$, then $u(\overline{\mathbf{q}})=0$ and we obtain similarly to (50)

$$\overline{M}_{\lambda,\delta} = \lambda U_h(\overline{\mathbf{p}})-\frac{1}{2\delta}\|\overline{\mathbf{p}}-\overline{\mathbf{q}}\|^2 \le U_h(\overline{\mathbf{p}}) \le C_{\mathrm{bd}} d_{\partial\Omega}(\overline{\mathbf{p}})+C'_{\mathrm{bd}}h \le 4C_{\mathrm{Lip}}C_{\mathrm{bd}}\delta+C'_{\mathrm{bd}}h.$$

We used the same arguments as in (50), except for the second inequality which is based on assumption (ii) of Theorem 2.3. Likewise, if $\tilde{\mathbf{q}}\in\mathbb{E}\setminus\Omega$ then $\widetilde{M}_{\lambda,\delta}\le -U_h(\tilde{\mathbf{p}})\le C_{\mathrm{bd}}(h+4C_{\mathrm{Lip}}\delta)$.

Following assumption (i) of Theorem 2.3, we assume that $(\overline{\mathbf{p}},\overline{\mathbf{q}})\notin\Omega_h\times\Omega$, thus either $\overline{\mathbf{p}}\notin\Omega_h$ or $\overline{\mathbf{q}}\notin\Omega$, which yields by the above arguments

$$\overline{M}_{\lambda,\delta}\le\max\{4C_{\mathrm{Lip}}^2\delta, 4C_{\mathrm{Lip}}C_{\mathrm{bd}}\delta+C'_{\mathrm{bd}}h\}.$$

Likewise for $\widetilde{M}_{\lambda,\delta}$ using the assumption that $(\tilde{\mathbf{p}},\tilde{\mathbf{q}})\notin\Omega_h\times\Omega$. The announced result (25) follows from Lemma C.2 and the these bounds on $\overline{M}_{\lambda,\delta}$ and $\widetilde{M}_{\lambda,\delta}$.

References

[1] Ken Alton and Ian M Mitchell. An Ordered Upwind Method with Precomputed Stencil and Monotone Node Acceptance for Solving Static Convex Hamilton-Jacobi Equations. *Journal of Scientific Computing*, 51(2):313–348, July 2011.

[2] M Bardi and I Capuzzo-Dolcetta. Optimal control and viscosity solutions of Hamilton-Jacobi-Bellman equations. Bikhauser, 1997.

[3] Jean-David Benamou, Francis Collino, and Jean-Marie Mirebeau. Monotone and Consistent discretization of the Monge-Ampere operator. *Mathematics of computation*, September 2015.

[4] Fethallah Benmansour and Laurent D. Cohen. Tubular Structure Segmentation Based on Minimal Path Method and Anisotropic Enhancement. *International Journal of Computer Vision*, 92(2):192–210, March 2010.

[5] Folkmar Bornemann and Christian Rasch. Finite-element Discretization of Static Hamilton-Jacobi Equations based on a Local Variational Principle. *Computing and Visualization in Science*, 9(2):57–69, June 2006.

[6] D Chen, Jean-Marie Mirebeau, and L D Cohen. Global Minimum for Curvature Penalized Minimal Path Method. *BMVC*, 2015.

[7] Da Chen. *New Minimal Path Models for Tubular Structure Extraction and Image Segmentation*. PhD thesis, University Paris-Dauphine, September 2016.

[8] Da Chen, Laurent D. Cohen, and Jean-Marie Mirebeau. Vessel Extraction Using Anisotropic Minimal Paths and Path Score. In *IEEE International Conference on Image Processing (ICIP 2014)*, paris, France, 2014. IEEE.

[9] J H Conway and N J A Sloane. Low-Dimensional Lattices. III. Perfect Forms. *Proceedings of the Royal Society of London A: Mathematical, Physical and Engineering Sciences*, 418(1854):43–80, July 1988.

[10] J H Conway and N J A Sloane. Low-Dimensional Lattices. VI. Voronoi Reduction of Three-Dimensional Lattices. *Proceedings of the Royal Society A: Mathematical, Physical and Engineering Sciences*, 436(1896):55–68, January 1992.

[11] Michael G Crandall and Pierre-Louis Lions. Viscosity solutions of Hamilton-Jacobi equations. *Transactions of the American Mathematical Society*, 277(1):1–42, 1983.

[12] Remco Duits, Stephan P L Meesters, Jean-Marie Mirebeau, and Jorg M Portegies. Optimal Paths for Variants of the 2D and 3D Reeds-Shepp Car with Applications in Image Analysis. *arXiv.org*, December 2016.

[13] Lawrence C Evans. *Partial Differential Equations*. American Mathematical Soc., 2010.

[14] Jérôme Fehrenbach and Jean-Marie Mirebeau. Sparse Non-negative Stencils for Anisotropic Diffusion. *Journal of Mathematical Imaging and Vision*, pages 1–25, 2013.

[15] R Kimmel and J. A. Sethian. Computing geodesic paths on manifolds. *Proceedings of the National Academy of Sciences*, 95(15):8431–8435, July 1998.

[16] J L Lagrange. *Recherches d'arithmétique*. C.F. Voss, 1775.

[17] Jean-Marie Mirebeau. Efficient fast marching with Finsler metrics. *Numerische Mathematik*, pages 1–43, 2013.

[18] Jean-Marie Mirebeau. Anisotropic Fast-Marching on cartesian grids using Lattice Basis Reduction. *SIAM Journal on Numerical Analysis*, 52(4):1573–1599, January 2014.

[19] Jean-Marie Mirebeau. Minimal stencils for discretizations of anisotropic PDEs preserving causality or the maximum principle. *SIAM Journal on Numerical Analysis*, 54(3):1582–1611, 2016.

[20] Richard Montgomery. *A Tour of Subriemannian Geometries, Their Geodesics and Applications*. American Mathematical Soc., August 2006.

[21] A M Oberman. Convergent Difference Schemes for Degenerate Elliptic and Parabolic Equations: Hamilton–Jacobi Equations and Free Boundary Problems. *SIAM Journal on Numerical Analysis*, 44(2):879–895, January 2006.

[22] Gabriel Peyré, Mickael Péchaud, Renaud Keriven, and Laurent D. Cohen. *Geodesic Methods in Computer Vision and Graphics*.

[23] Gunnar Randers. On an Asymmetrical Metric in the Four-Space of General Relativity. *Physical Review*, 59(2):195–199, January 1941.

[24] Elisabeth Rouy and Agnès Tourin. A Viscosity Solutions Approach to Shape-From-Shading. *SIAM Journal on Numerical Analysis*, 29(3):867–884, July 1992.

[25] Gonzalo Sanguinetti, Erik Bekkers, Remco Duits, Michiel H J Janssen, Alexey Mashtakov, and Jean-Marie Mirebeau. Sub-Riemannian fast marching in SE(2). In *Progress in Pattern Recognition, Image Analysis, Computer Vision, and Applications*, pages 366–374. Springer, Cham, Cham, 2015.

[26] A Schürmann. Computational geometry of positive definite quadratic forms. *University Lecture Series*, 2009.

[27] Eduard Selling. Ueber die binären und ternären quadratischen Formen. *Journal fur die Reine und Angewandte Mathematik*, 77:143–229, 1874.

[28] J. A. Sethian. Level Set Methods and Fast Marching Methods: Evolving Interfaces in Computational Geometry, Fluid Mechanics, Computer Vision, and Materials Science. 1999.

[29] J. A. Sethian and A. Vladimirsky. Ordered upwind methods for static Hamilton-Jacobi equations. *Proceedings of the National Academy of Sciences of the United States of America*, 98(20):11069–11074 (electronic), 2001.

[30] James A. Sethian and Alexander Vladimirsky. Ordered upwind methods for static Hamilton-Jacobi equations: theory and algorithms. *SIAM Journal on Numerical Analysis*, 41(1):325–363, 2003.

[31] Alex Shum, Kirsten Morris, and Amir Khajepour. Convergence Rate for the Ordered Upwind Method. *arXiv.org*, (3):889–913, January 2016.

[32] Alon Spira and Ron Kimmel. An efficient solution to the eikonal equation on parametric manifolds. *Interfaces and Free Boundaries. Mathematical Modelling, Analysis and Computation*, 6(3):315–327, 2004.

[33] Petter Strandmark, Johannes Ulen, Fredrik Kahl, and Leo Grady. Shortest Paths with Curvature and Torsion. In *2013 IEEE International Conference on Computer Vision (ICCV)*, pages 2024–2031. IEEE, 2013.

[34] J.N. Tsitsiklis. Efficient algorithms for globally optimal trajectories. 40(9):1528–1538, September 1995.

[35] Alexander Vladimirsky. Label-setting methods for Multimode Stochastic Shortest Path problems on graphs. *Mathematics of Operations Research*, 33(4):821–838, 2008.

[36] Alexander Boris Vladimirsky. *Fast methods for static Hamilton-Jacobi Partial Differential Equations*. PhD thesis, May 2001.